Electronic Supplementary Information

for

Ditopic pillar[5]arene-based fluorescent enhancement material mediated by [*c*2]daisy chain formation**

Kai Wang,[a,b] Chun-Yu Wang,[a] Yumo Zhang,[a] Sean Xiao-An Zhang,*[a] Bing Yang[a] and Ying-Wei Yang*[a]

[*] K. Wang, C.-Y. Wang, Y. Zhang, Prof. Dr. S. X.-A. Zhang, Prof. B. Yang, Prof. Dr. Y.-W. Yang

[a]State Key Laboratory of Supramolecular Structure and Materials

College of Chemistry

Jilin University

2699 Qianjin Street, Changchun, Jilin 130012 P. R. China

Tel: (+86) 13009100930

Email: (Y.W.Y.) ywyang@jlu.edu.cn

[b]School of Chemistry and Environmental Engineering, Anyang Institute of Technology, Anyang, Henan 455000, China

[**] This research was supported by the National Natural Science Foundation of China (Grant No. 21272093), the Specialized Research Fund for the Doctoral Program of Higher Education of China (20120061120117), and the Innovation Program of the State Key Laboratory of Supramolecular Structrue and Materials.

Table of Contents

1. Materials and methods

Starting materials and reagents were purchased from Aldrich, Aladdin and Gibco, and used as received. All reagents were purchased from commercial sources and used without further purification, unless otherwise noted. Compound **G2** was prepared according to literature procedures.[S1] The products were purified by column chromatography over silica gel. ^{1}H-NMR and ^{13}C-NMR spectra were recorded at 25 ºC on a Bruker AVANCE III 300 MHz (or 500 MHz) and 125 MHz, respectively, and TMS was used as internal standard. Chemical shifts are reported in ppm relative to the signals corresponding to the residual non-deuterated solvent ($CDCl_3$: 7.260 ppm), and coupling constants were recorded in Hertz (Hz). The two-dimensional diffusion-ordered NMR spectra were recorded on a Bruker AVANCE 600 MHz. Mass spectra were recorded on Bruker Daltonics Autoflex Speed Series: High-Performance MALDI-TOF Systems. Ultraviolet-visible (UV-vis) spectra were recorded on a Shimadzu UV-2550 instrument. Fluorescence spectra were obtained with a Shimadzu spectrofuorimeter RF-5301 PC. All the theoretical calculations were performed using the Gaussian 09 program with b3lyp/6-31g(d,p). Then the vibrational spectrum of each molecule was calculated at the same level of theory to ensure that all structures correspond to true minima of the potential energy surface. The fluorescence lifetime was performed by the time-correlated single-photon counting (TCSPC) system using a mini-τ miniature fluorescence lifetime spectrometer (Edinburgh Instruments). A 375 nm picoseconds diode laser (Edinburgh Instruments EPL-375, repetition rate 20 MHz) was used to excite the samples, and the statistics was analyzed by reconvolution fit. The concentration of solution was kept at 10 μM.

2. Syntheses of compounds

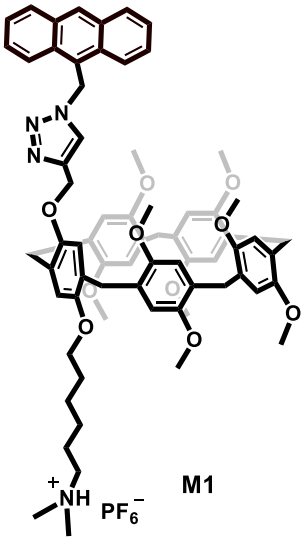

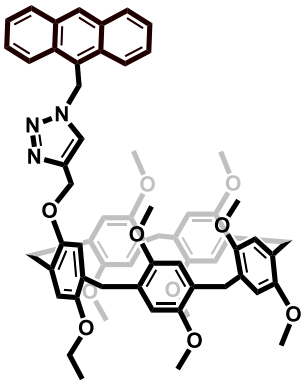

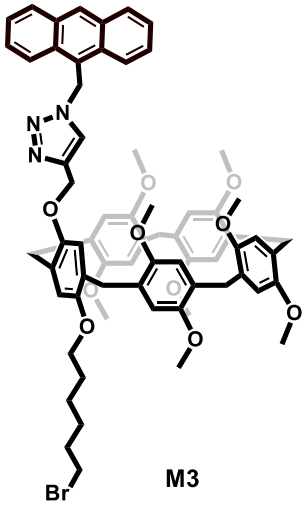

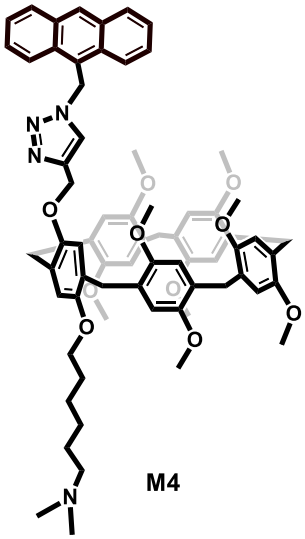

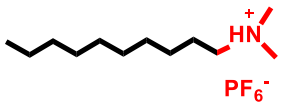

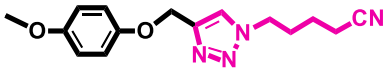

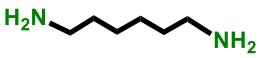

3. ^{1}H NMR spectra of M1

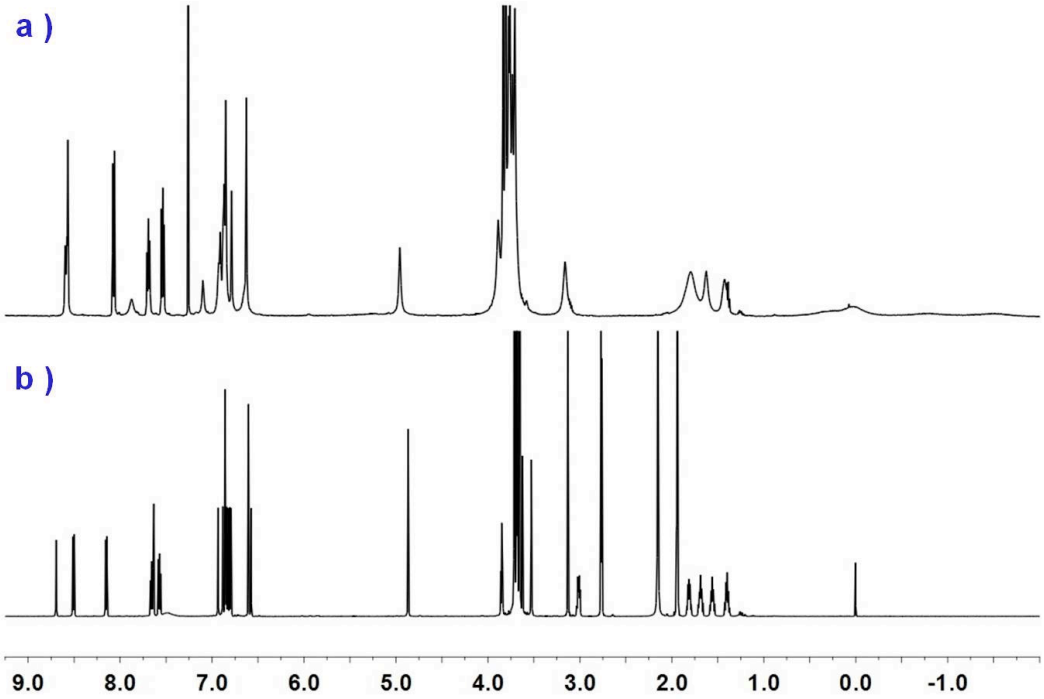

Figure S1. ^{1}H NMR spectra (500 mM, 298 K) of **M1** (5 mM) in different solvents: (a) $CDCl_3$, (b) CD_3CN.

4. Self-aggregation behavior of M1 in the diluted solution

Monomer-aggregate equilibrium equation in solution:[S2, S3]

$$n\ \text{Monomer} \xrightleftharpoons{K_{agg}} \text{aggregate}$$

C_{mon} C_{agg} C_{tot}

Where C_{tot}, C_{mon} and C_{agg} represent total, monomer and aggregate concentration; K_{agg} and n are aggregate constant and aggregate number, respectively.

$$K_{agg} = \frac{C_{agg}}{(C_{mon})^n}$$

$$C_{tot} = C_{mon} + nC_{agg}$$

$$\frac{C_{mon}}{C_{tot}} + \frac{nC_{agg}}{C_{tot}} = 1$$

$$\delta_{obs} = N_{mon}\delta_{mon} + N_{agg}\delta_{agg}$$

$$= \frac{C_{mon}}{C_{tot}}\delta_{mon} + \frac{nC_{agg}}{C_{tot}}\delta_{agg}$$

$$= (1 - \frac{nC_{agg}}{C_{tot}})\delta_{mon} + \frac{nC_{agg}}{C_{tot}}\delta_{agg}$$

$$\Rightarrow \delta_{obs} - \delta_{mon} = \frac{nC_{agg}}{C_{tot}}(\delta_{agg} - \delta_{mon})$$

$$\Rightarrow C_{agg} = \frac{\delta_{obs} - \delta_{mon}}{\delta_{agg} - \delta_{mon}} \cdot \frac{C_{tot}}{n}$$

$$K_{agg} = \frac{C_{agg}}{(C_{tot} - nC_{agg})^n}$$

$$\Rightarrow \ln K_{agg} = \ln C_{agg} - n\ln(C_{tot} - nC_{agg})$$

$$= \ln\frac{\delta_{obs} - \delta_{mon}}{\delta_{agg} - \delta_{mon}} \cdot \frac{C_{tot}}{n} - n\ln(C_{tot} - n \cdot \frac{\delta_{obs} - \delta_{mon}}{\delta_{agg} - \delta_{mon}} \cdot \frac{C_{tot}}{n})$$

$$= \ln\frac{\delta_{obs} - \delta_{mon}}{\delta_{agg} - \delta_{mon}} \cdot \frac{C_{tot}}{n} - n\ln\frac{\delta_{agg} - \delta_{obs}}{\delta_{agg} - \delta_{mon}} \cdot C_{tot}$$

$$= \ln\frac{\delta_{obs} - \delta_{mon}}{\delta_{agg} - \delta_{mon}} \cdot C_{tot} - \ln n - n\ln\frac{\delta_{agg} - \delta_{obs}}{\delta_{agg} - \delta_{mon}} \cdot C_{tot}$$

$\Rightarrow$

$$\ln K_{agg} + \ln n = \ln(\delta_{mon} - \delta_{obs})C_{tot} - \ln\left(\delta_{mon} - \delta_{agg}\right) - n\ln(\delta_{obs} - \delta_{agg})C_{tot} + n\ln(\delta_{mon} - \delta_{agg})$$

$\Rightarrow$

$$\ln(\delta_{mon} - \delta_{obs})C_{tot} = n\ln(\delta_{obs} - \delta_{agg})C_{tot} + \ln K_{agg} + \ln n - (n-1)\ln(\delta_{mon} - \delta_{agg}) \qquad \text{(I)}$$

Substitute n = 2 in the monomer-aggregate equation gives the monomer-dimer equilibrium equation as follow:

$$\delta_{obs} = \delta_{dimer} + \{(\delta_{mon} - \delta_{dimer})[-1 + (1 + 8\,K_{dimer}C_{tot})^{1/2}]/(4\,K_{dimer}C_{tot})\} \qquad \text{(II)}$$

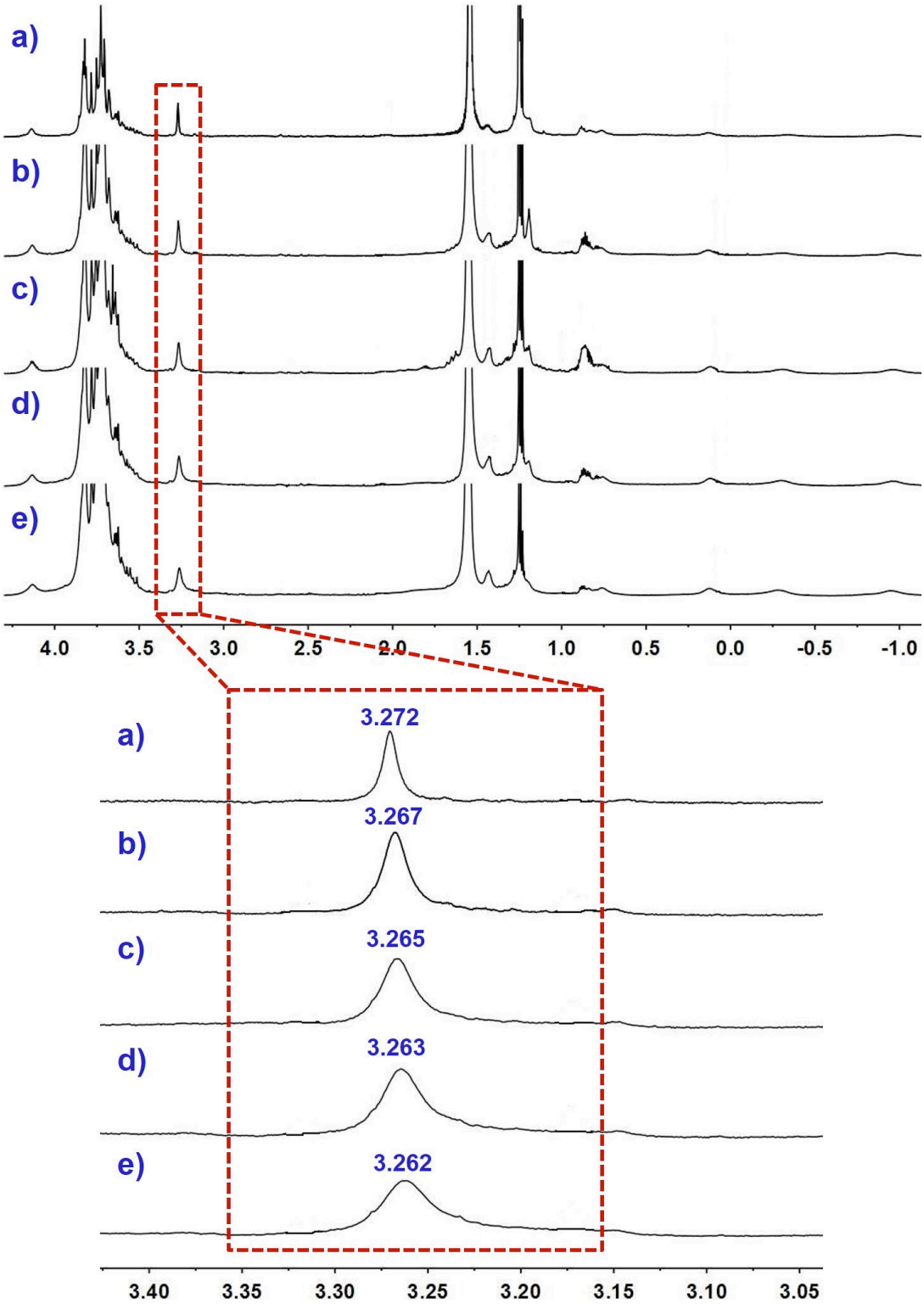

Figure S2. ^{1}H NMR (500 MHz, $CDCl_3$, 298 K) spectra of **M1** at low concentrations (the concentration refers to the total concentration of initial **M1**). From up to bottom: (a) 0.19 mM, (b) 0.40 mM, (c) 0.61 mM, (d) 0.81 mM and (e) 1.00 mM.

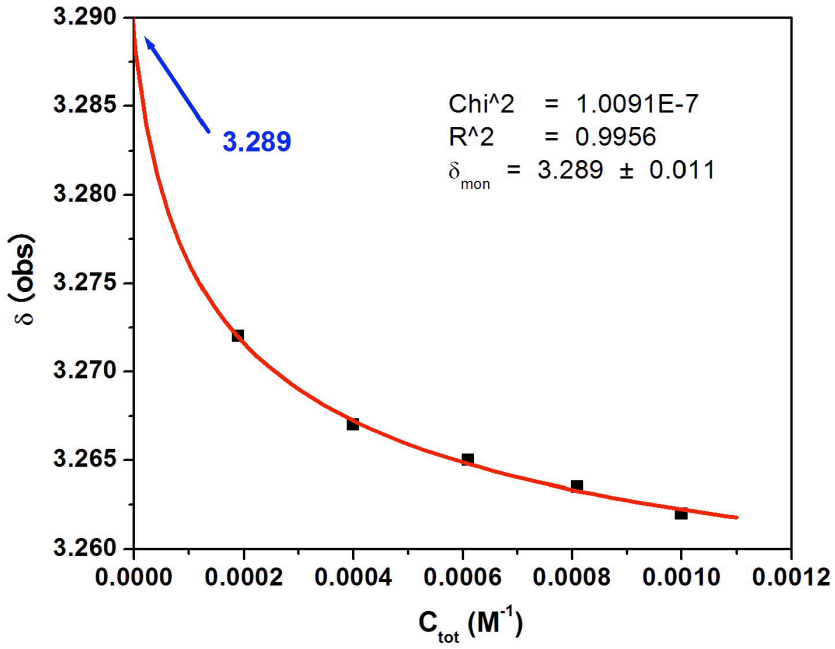

Figure S3. Plot of chemical shift (δ_{obs}) *vs* the total concentration (C_{tot}) of **M1** for δ_{mon}. The chemical shift that is plotted here (δ_{obs}) is that data shown in Figure S2. Dots are experimental data and the curve is obtained through non-linear fitting of data according to equation (II).

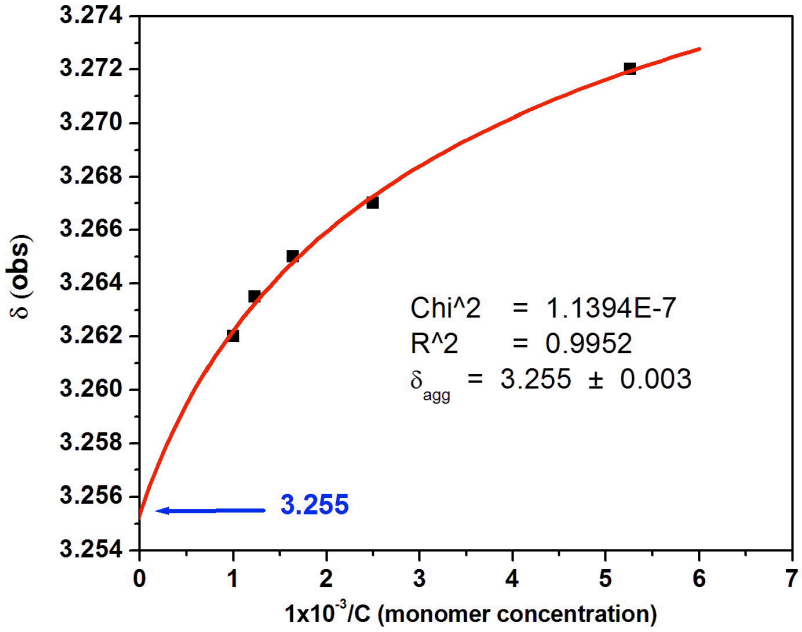

Figure S4. Plot of chemical shift (δ_{obs}) *vs* the reciprocal of the total concentration (C_{tot}) of **M1** for δ_{agg}. Dots are experimental data and the curve is best fit. The value 3.255 was obtained from equation (II) through non-linear fitting based on the data in Figure S2.

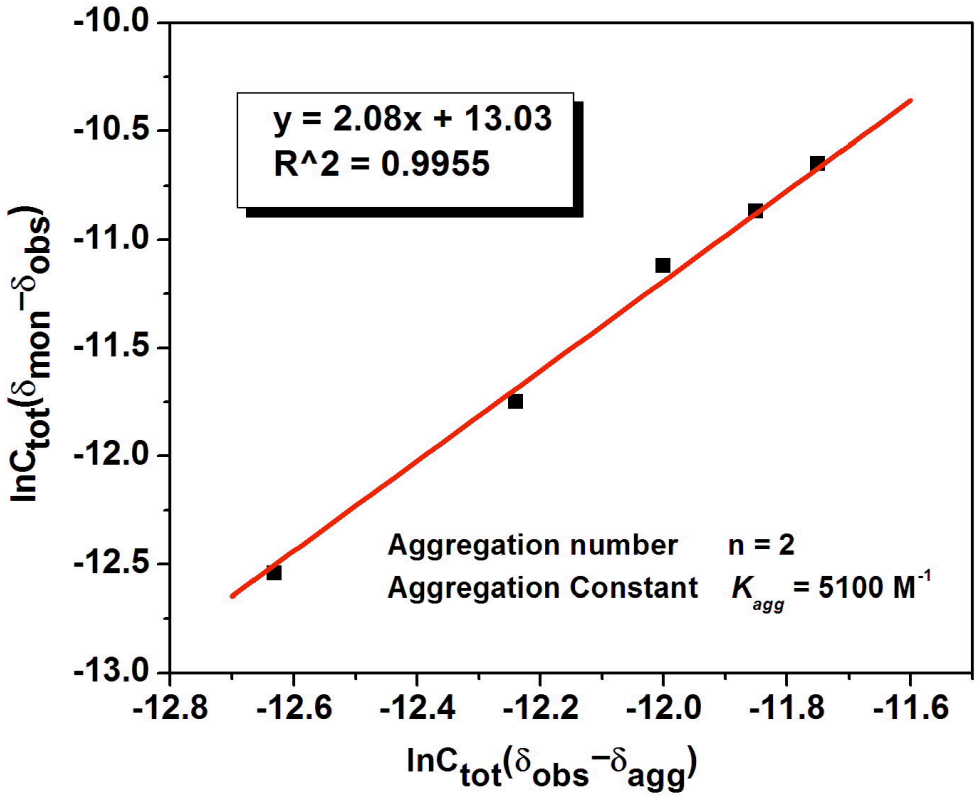

Figure S5. Plots from ^{1}H NMR data of **M1** as a function of total concentration to determine the aggregation equilibrium constant and aggregation number. Plots of $\ln[C_{tot}\ (\delta_{mon} - \delta_{obs})]$ *vs.* $\ln[C_{tot}\ (\delta_{obs} - \delta_{agg})]$ give a straight line, from which the slope and the intercept can be calculated to yield n and K_{agg} according to equation (I).

According to equation (I), aggregation number n and self-aggregation constant K_{agg} can be obtained, where C_{tot} refers to the total concentration of initial **M1**, δ_{mon} and δ_{agg} refers the extrapolated values of the monomer and aggregate, respectively. By plotting δ_{obs} against the total concentration and extrapolating to zero **M1** concentration, the chemical shift of the monomer (δ_{mon}) can be estimated graphically from equation (II) (Fig. S3). Extrapolation of the concentration to infinity yields the chemical shift of the aggregate (δ_{agg}) (Fig. S4). Plots of $\ln[C_{tot}\ (\delta_{mon} - \delta_{obs})]$ *vs.* $\ln[C_{tot}\ (\delta_{obs} - \delta_{agg})]$ give a straight line, from which the slope and the intercept can be calculated to yield n = 2 and K_{agg} = 5100 M^{-1} according to equation (I) (Fig. S5).

5. Selectivity and guest-dependent fluorescent enhancement of M2

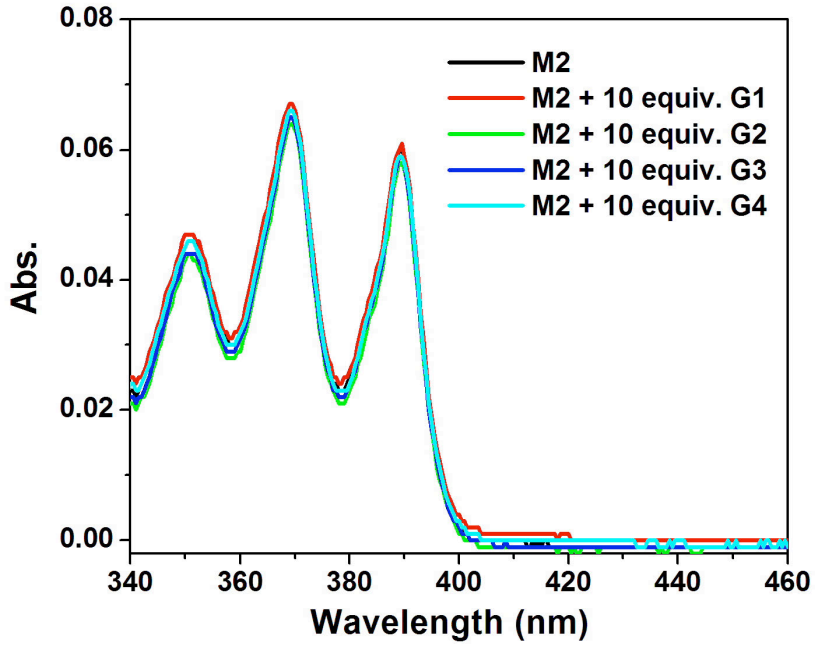

Figure S6. Absorption spectra of **M2** (10 μM) upon the addition of different guests in chloroform.

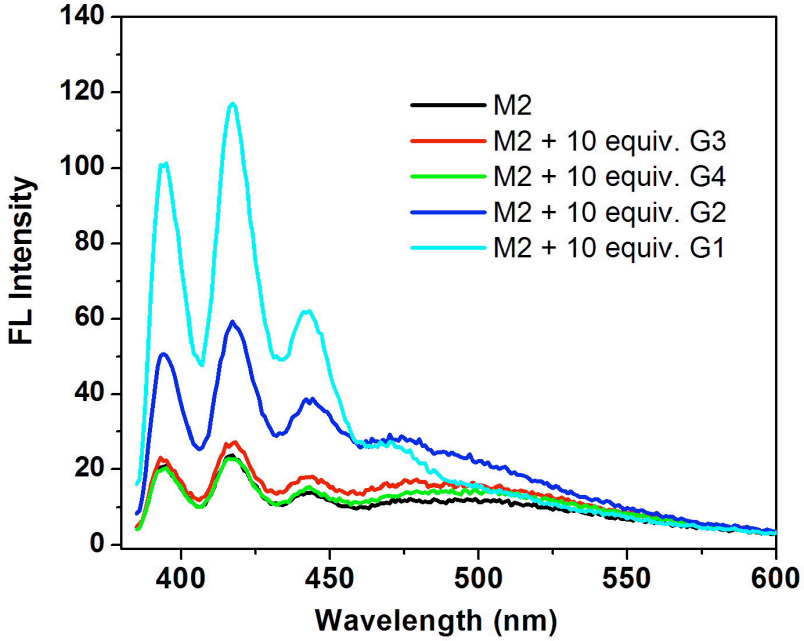

Figure S7. Fluorescent emission spectra of **M2** (10 μM) upon the addition of different guests in chloroform. λ_{ex} = 370 nm; slit widths (ex: 1.5 nm, em: 3 nm).

6. Stoichiometry and association constant determination for the complexation between M2 and G1

The association constant (K_a) of **M2** and **G1** was determined by fluorescent titration experiment. The fluorescent titration experiments were carried out by measuring the emission intensity (at 417 nm) upon excitation at 370 nm. The stoichiometry of the complex was determined using the Job plot method based on the changes of fluorescent emission intensity according to the literature.[S4]

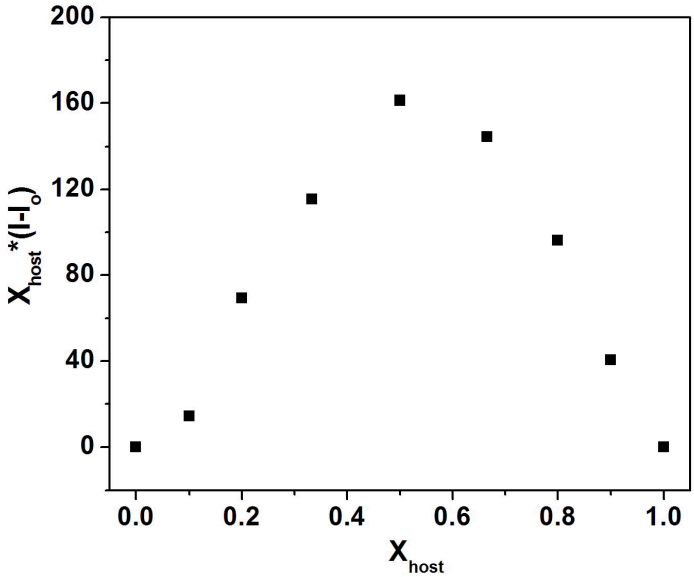

Figure S8. Job plot of **M2** and **G1**.

The titration experiments were performed with a constant concentration of **M2** (1×10^{-5} M) and varying concentrations of **G1** in chloroform. Binding constants were determined by plotting changes in ratios (I/I_o) of the emission intensity at 417 nm versus the concentration of guest based on the following equation:

$$\frac{I}{I_o} = \frac{1 + \alpha K_a C_{guest}}{1 + K_a C_{guest}}$$

Where I is the intensity of fluorescent emission at 417 nm, I_o is the fluorescent intensity of free host , "α" is a constant , K_a is the binding constant, and C_{guest} is the total concentration of guest.[S5]

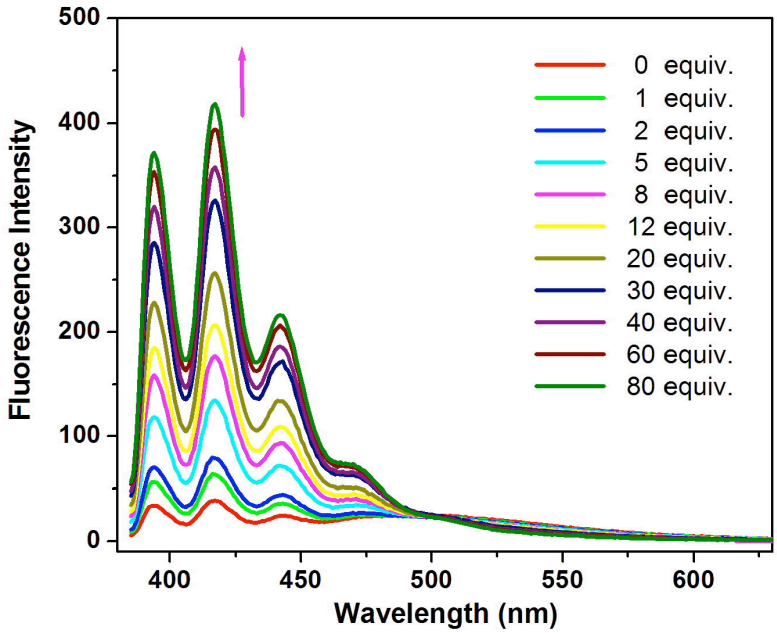

Figure S9. Fluorescent titrations of **M2** (10 μM) with different equivalent of **G1** in chloroform. λ_{ex} = 370 nm; slit widths (ex: 3 nm, em: 3 nm).

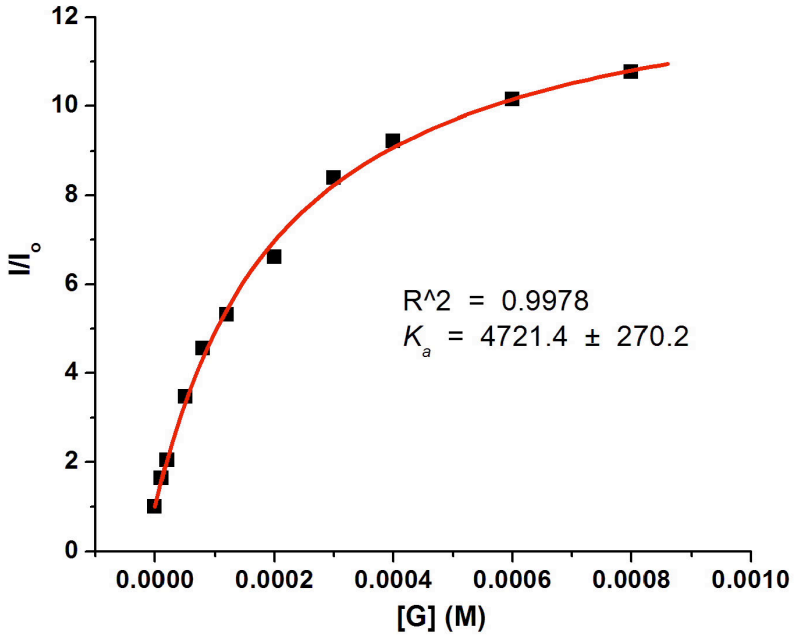

Figure S10. Curve-fitting plot for the ratio changes of fluorescent intensities at 417 nm of **M2** upon the addition of **G1**.

7. COSY spectra of M1 and M2

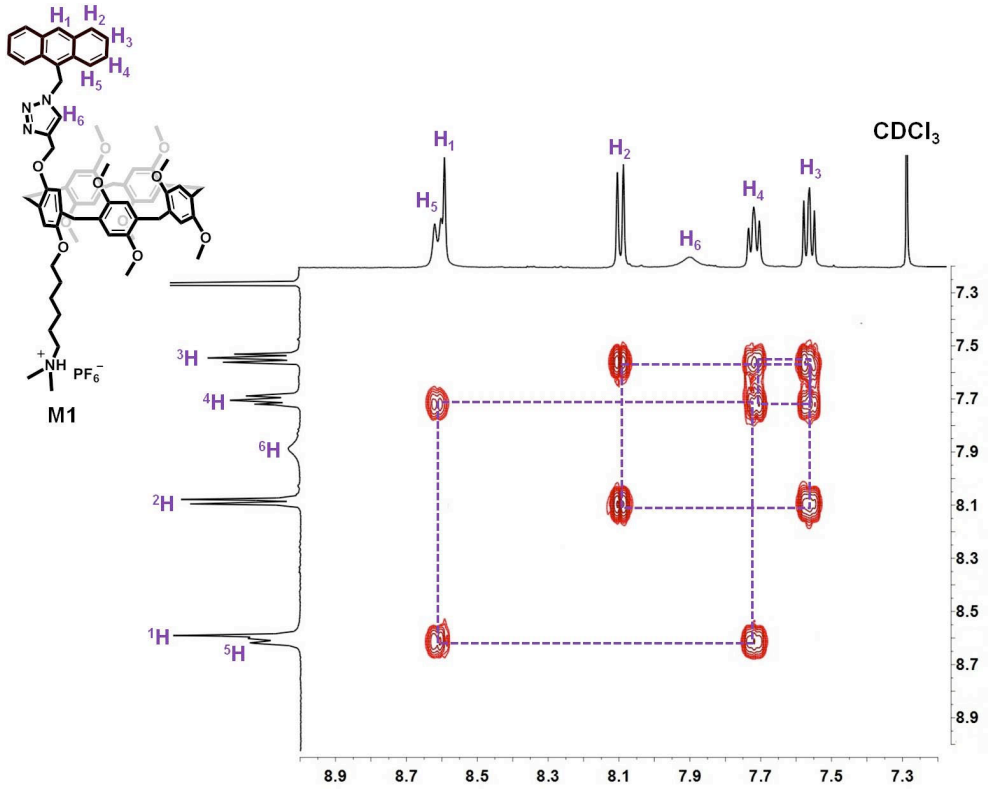

Figure S11. Partial 2D COSY spectrum (500 MHz, $CDCl_3$, 298 K) of **M1** (5 mM).

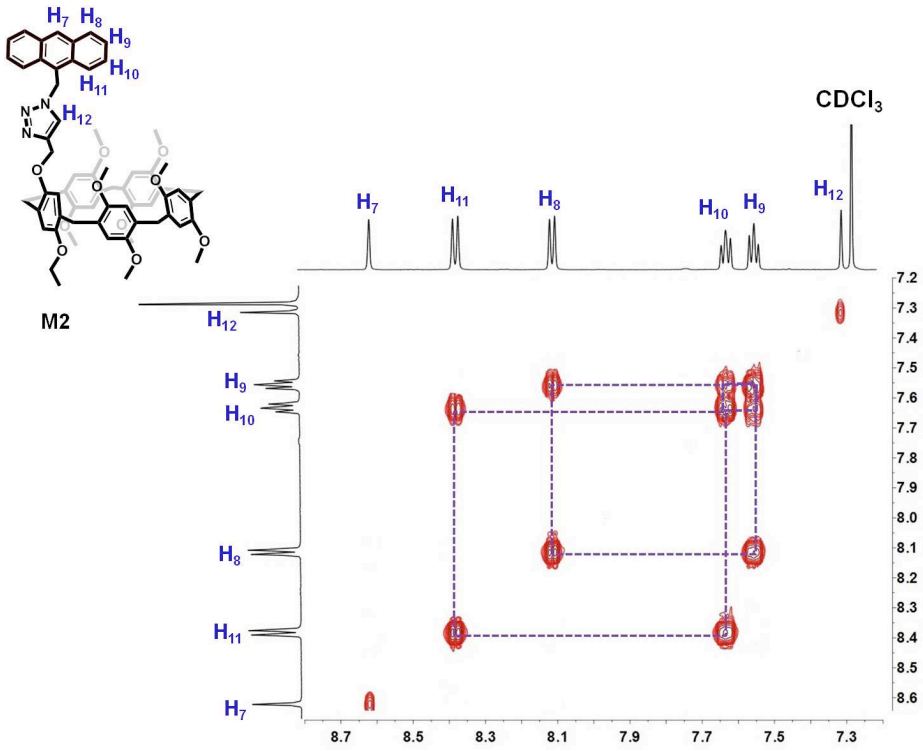

Figure S12. Partial 2D COSY spectrum (500 MHz, $CDCl_3$, 298 K) of **M2** (5 mM).

8. ROESY spectra of M1 and M2

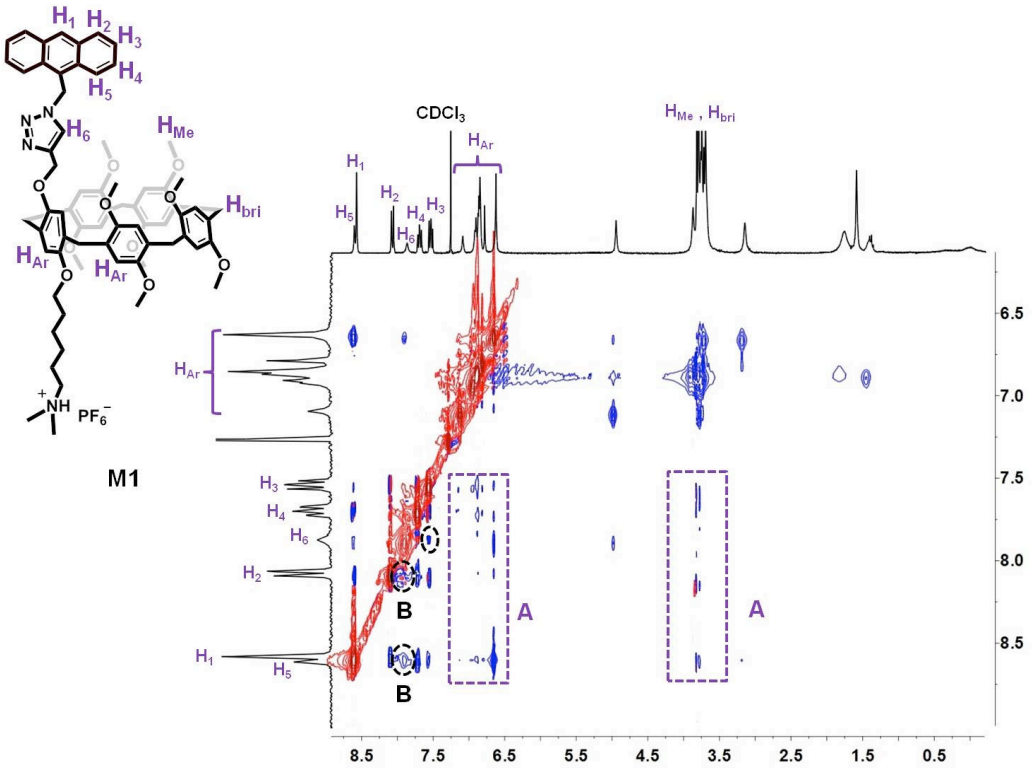

Figure S13. Partial 2D ROESY spectrum (500 MHz, $CDCl_3$, 298 K) of **M1** (5 mM).

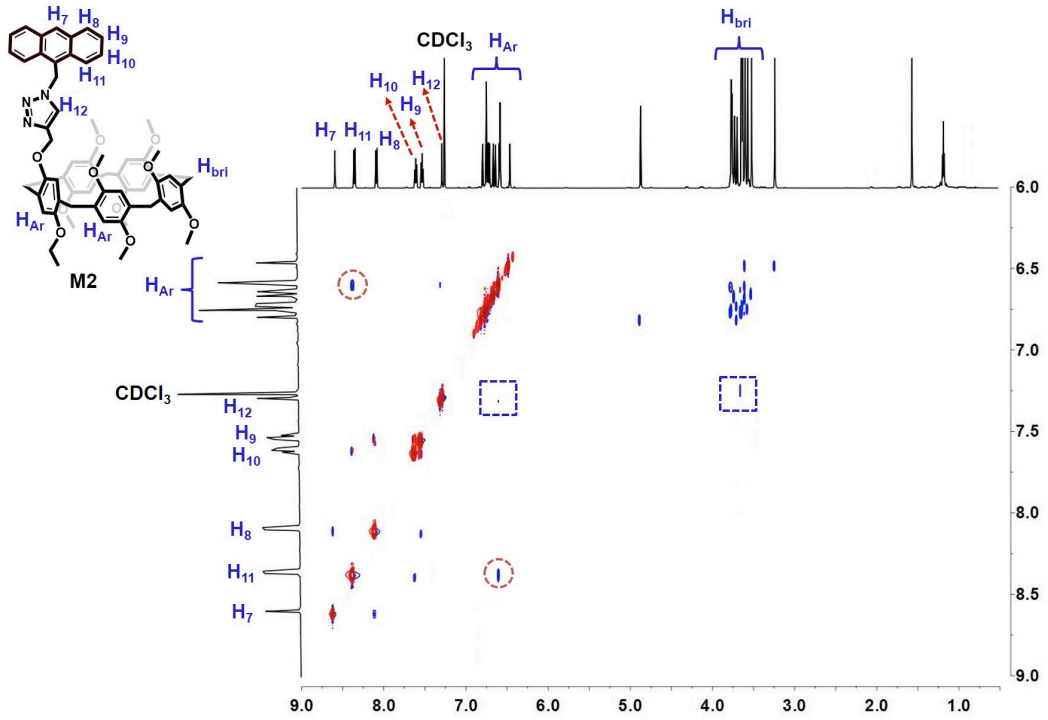

Figure S14. Partial 2D ROESY spectrum (500 MHz, $CDCl_3$, 298 K) of **M2** (5 mM).

9. Fluorescence quantum yield measurements

Fluorescence quantum yields (QYs) were estimated using argon saturated solutions of anthracene in ethanol ($\Phi_F = 0.28$, excitation at 360 nm) as a standard.[S6] The QYs were determined by comparing the integrated fluorescence intensity (excited at 370 nm for **M1**) and the absorbance value (less than 0.1 at the excitation wavelength). The slope method[S7] was used to calculate the QYs of compound **M1** and **M2** using the equation:

$$\Phi_x = \Phi_{st}(K_x/K_{st})(\eta_x/\eta_{st})^2$$

Where Φ is the quantum yield, K is the slope determined by the curves and η is the refractive index of the corresponding solution. The subscript "*st*" refers to the standards and "*x*" refers to the unknown samples.

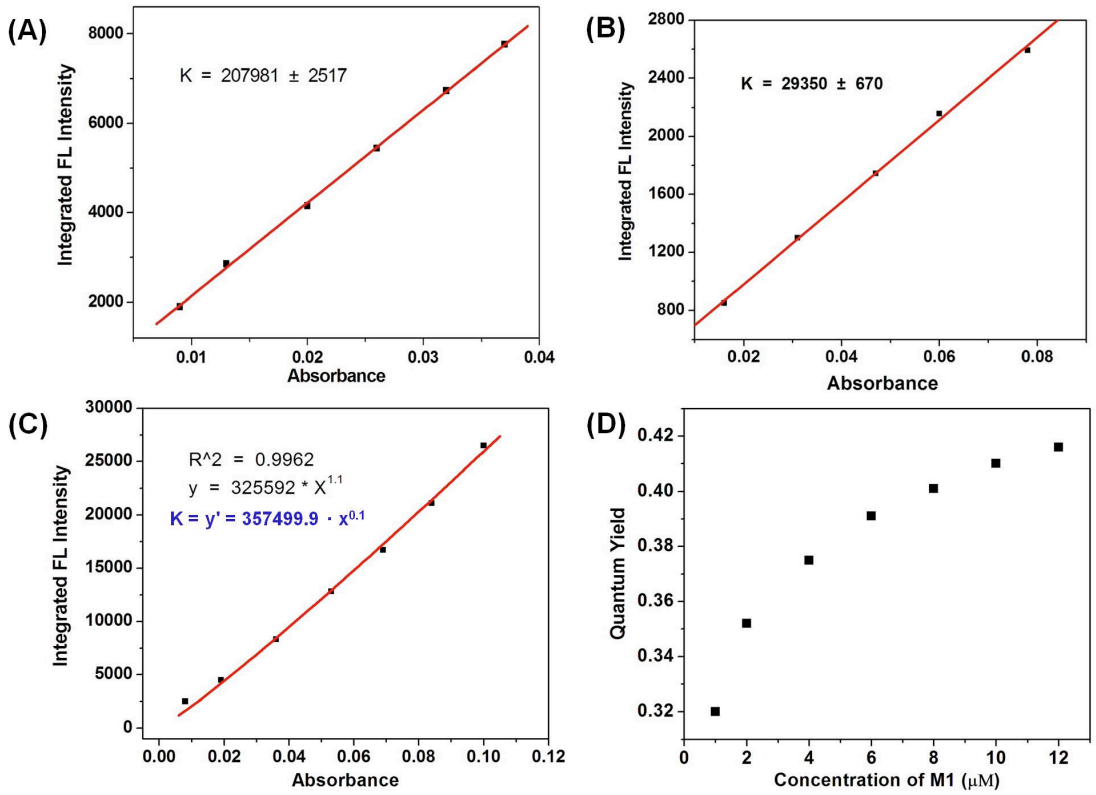

Figure S15. Fluorescence and absorbance of the anthracene in ethanol (A), **M2** in chloroform (B), **M1** in chloroform (C). As the concentration of **M1** increases in choloroform, its quantum yield increases accordingly (D).

10. Stimuli-responsive behaviours of M1

10.1 Thermal-responsiveness

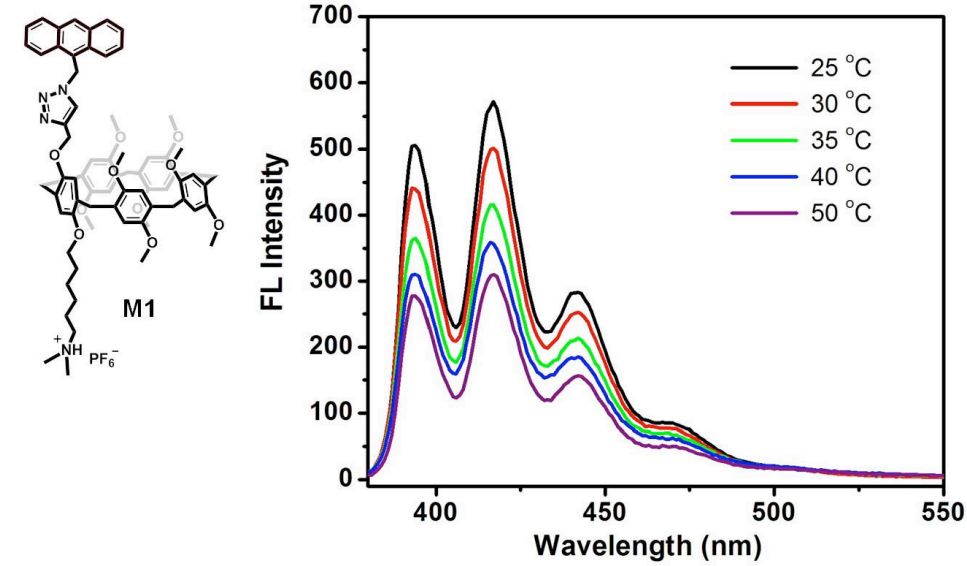

Figure S16. Fluorescence emission spectra of **M1** (10 μM in chloroform) at different temperatures. λ_{ex} = 370 nm; slit widths (1.5 nm, 3 nm).

10.2 pH-Responsiveness

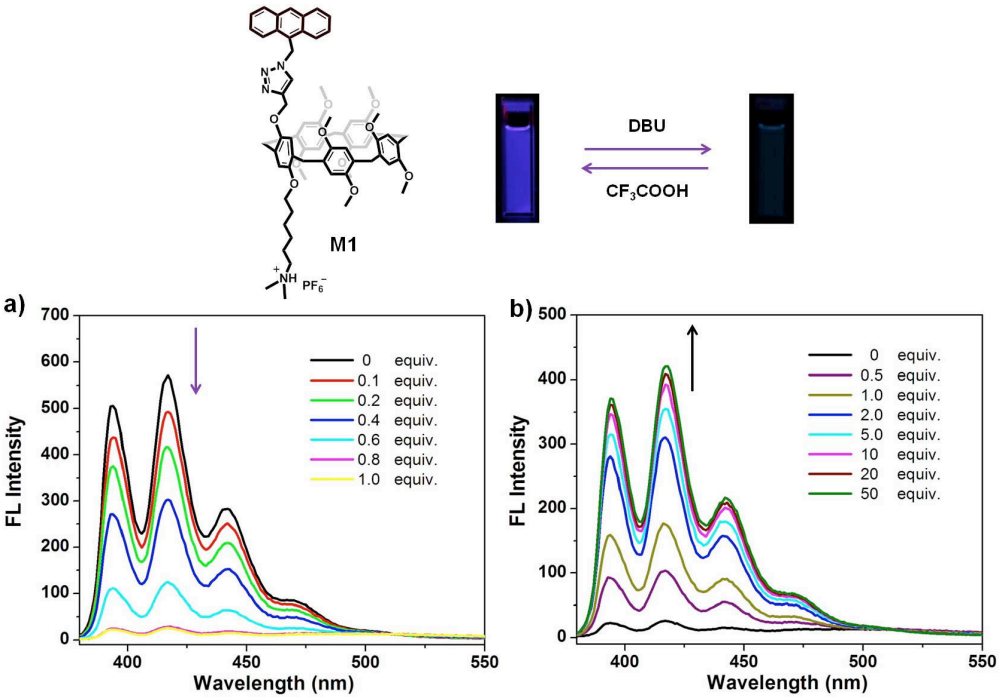

Figure S17. (a) Fluorescence spectra of **M1** (10 μM in $CHCl_3$) in the presence of different amounts of DBU (from 0 to 1.0 equiv.). (b) Fluorescence spectra of **M1** (10 μM) and DBU (10 μM) in $CHCl_3$ upon the addition of different amounts of CF_3COOH (from 0 to 50 equiv.). λ_{ex} = 370 nm; slit widths (ex: 1.5 nm, em: 3 nm).

10.3 Anion-responsiveness

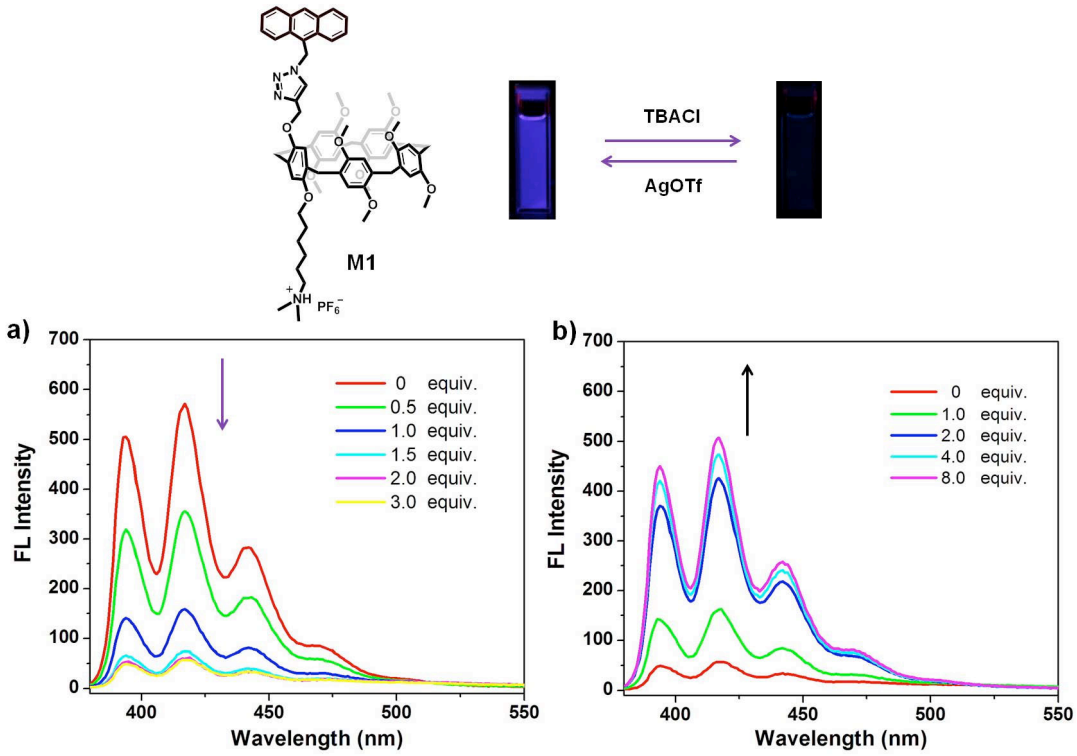

Figure S18. (a) Fluorescence spectra of **M1** (10 μM in $CHCl_3$) in the presence of different amounts of TBACl (from 0 to 3.0 equiv.). (b) Fluorescence spectra of **M1** (10 μM) and TBACl (20 μM) in $CHCl_3$ upon the addition of different amounts of AgOTf (from 0 to 8.0 equiv.). λ_{ex} = 370 nm; slit widths (ex: 1.5 nm, em: 3 nm).

10.4 Fluorescence spectra of anthracene under external stimuli

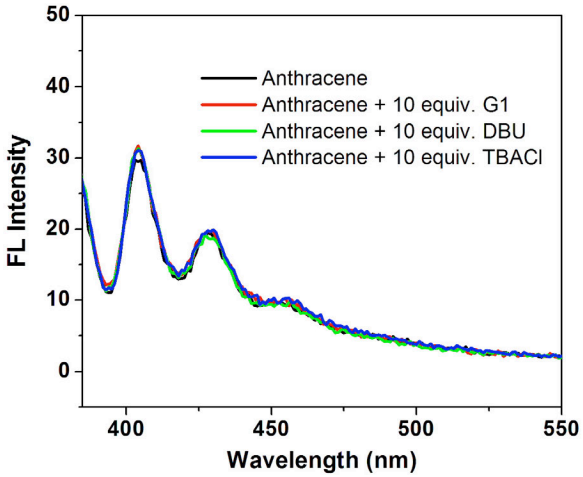

Figure S19. Fluorescence spectra of anthracene (10 μM in $CHCl_3$) in the presence of **G1** (red line), DBU (green line) and TBACl (blue line). The fluorescence intensities exhibit no change under these conditions. λ_{ex} = 370 nm; slit widths (ex: 1.5 nm, em: 3 nm).

10.5 ^{1}H NMR spectra of complexation-decomplexation ([*c*2]daisy chain-monomer) transitions of M1

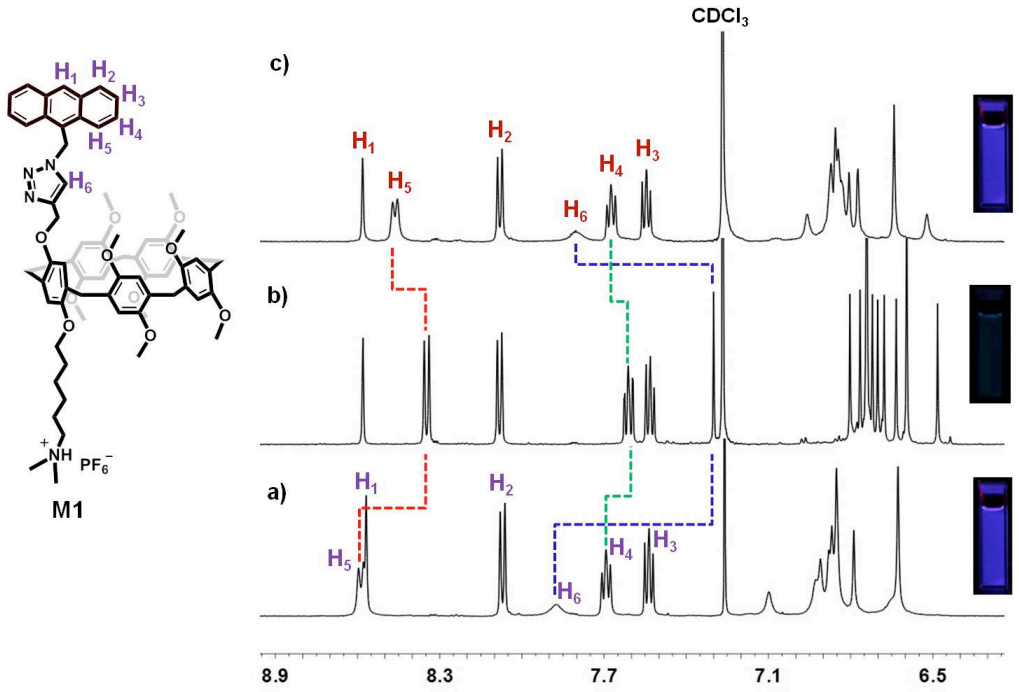

Figure S20. Partial ^{1}H NMR spectra (500 MHz, $CDCl_3$, 298 K): a) **M1**; b) a solution of 1.0 mM **M1** and 1.0 mM DBU; c) a solution of 1.0 mM **M1**, 1.0 mM DBU and 3.0 mM CF_3COOH. The photographic images clearly show the high-contrast fluorescence switching.

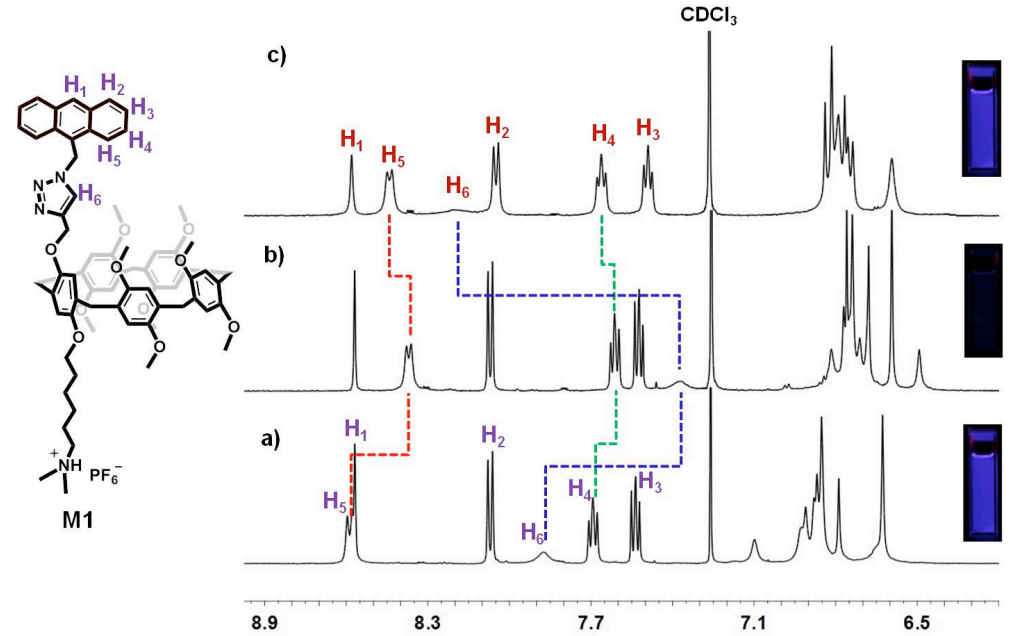

Figure S21. Partial ^{1}H NMR spectra (500 MHz, $CDCl_3$, 298 K): a) **M1**; b) a solution of 1.0 mM **M1** and 1.2 mM TBACl; c) a solution of 1.0 mM **M1**, 1.2 mM TBACl and 3.0 equiv. AgOTf. The photographic images clearly show the high-contrast fluorescence switching.

10.6 Switchable behaviors of [*c*2]daisy chain-monomer of M1 investigated by DOSY experiments

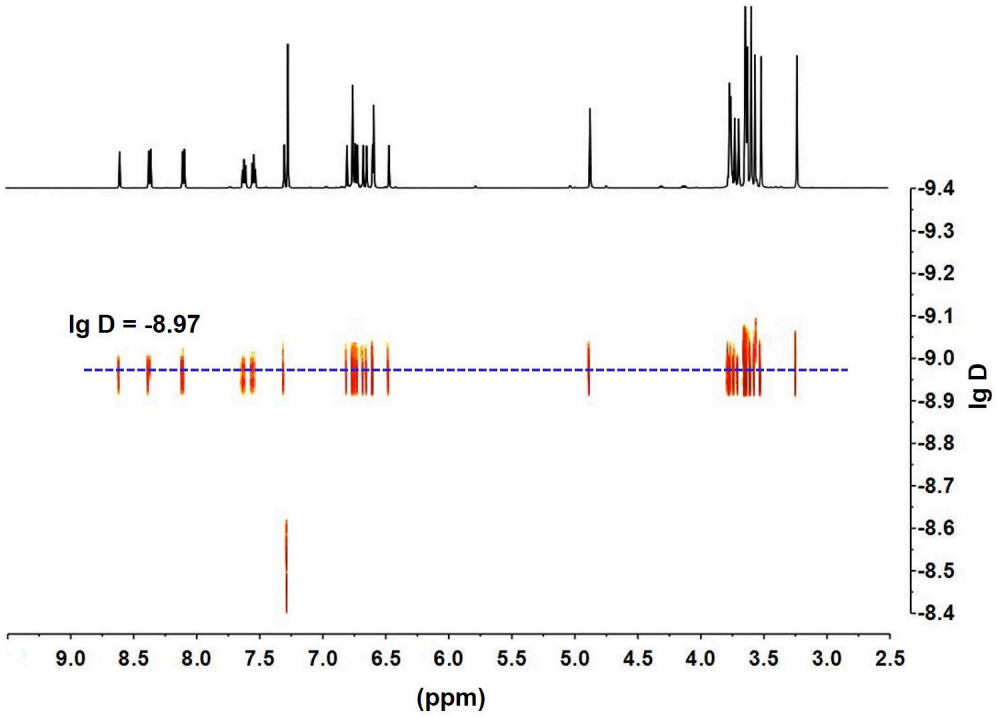

Figure S22. The diffusion coefficient (lg D) (600 MHz, $CDCl_3$, 298K) spectrum of **M2** (2 mM).

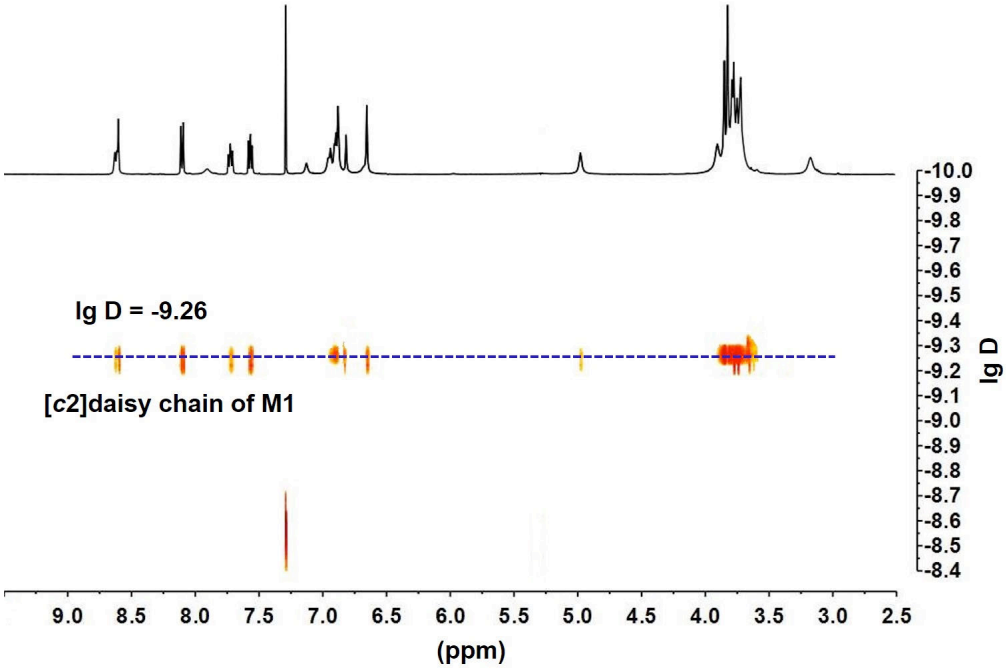

Figure S23. The diffusion coefficient (lg D) (600 MHz, $CDCl_3$, 298K) spectrum of **M1** (2 mM).

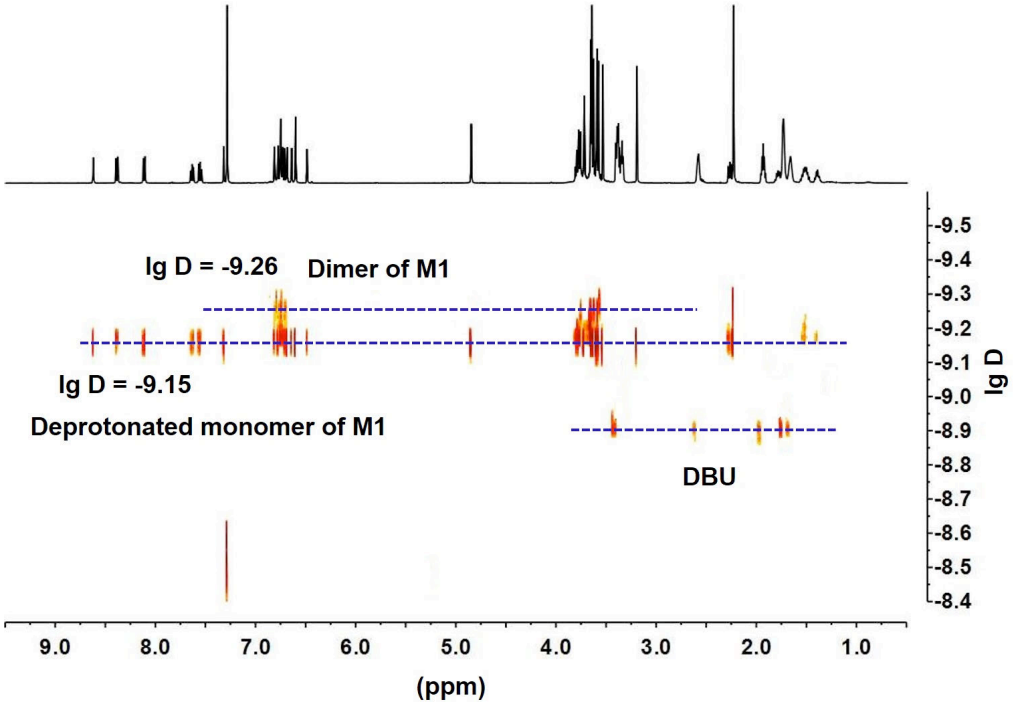

Figure S24. The diffusion coefficient (lg D) (600 MHz, $CDCl_3$, 298K) spectrum of **M1** (2 mM) and DBU (2 mM).

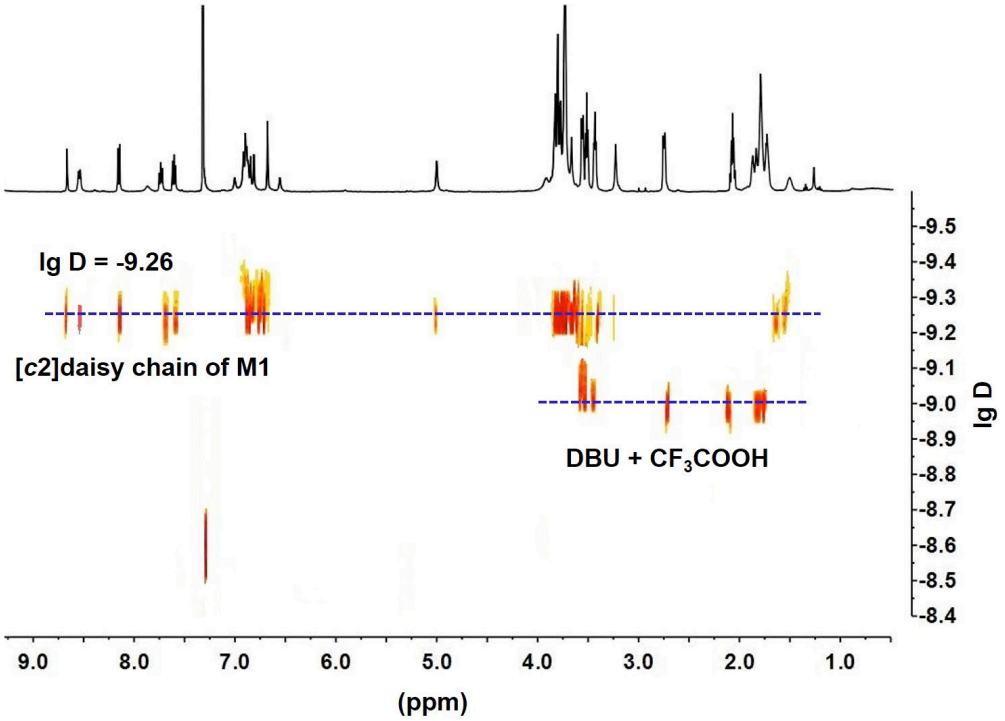

Figure S25. The diffusion coefficient (lg D) (600 MHz, $CDCl_3$, 298K) spectrum of **M1** (2 mM), DBU (2 mM) and CF_3COOH (10 mM).

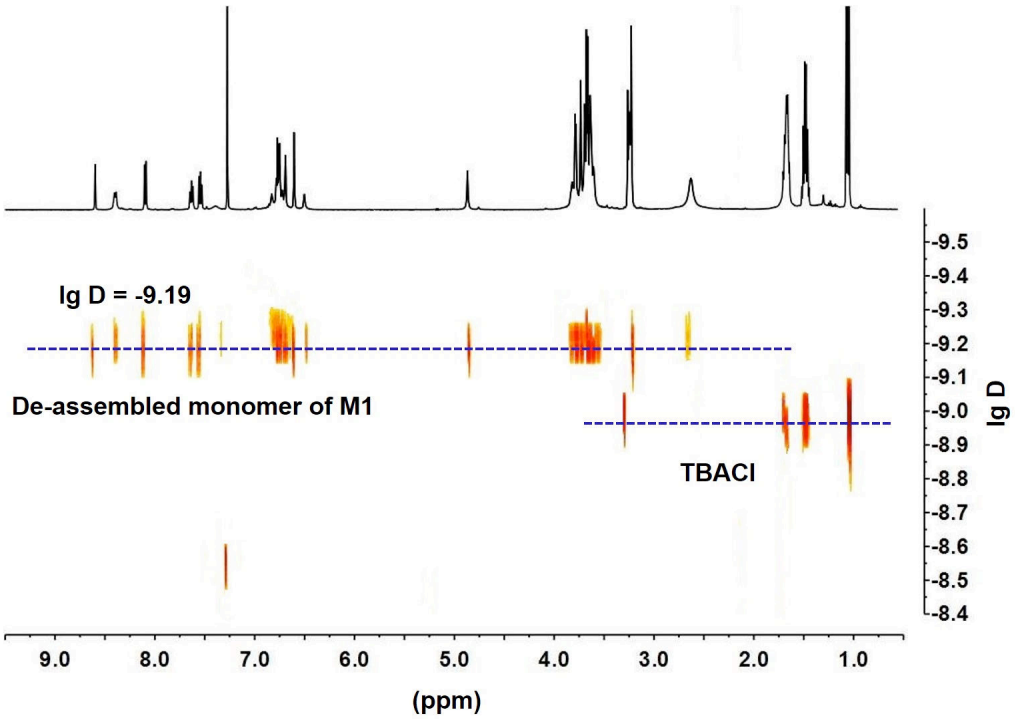

Figure S26. The diffusion coefficient (lg D) (600 MHz, $CDCl_3$, 298K) spectrum of **M1** (2 mM) and TBACl (4 mM).

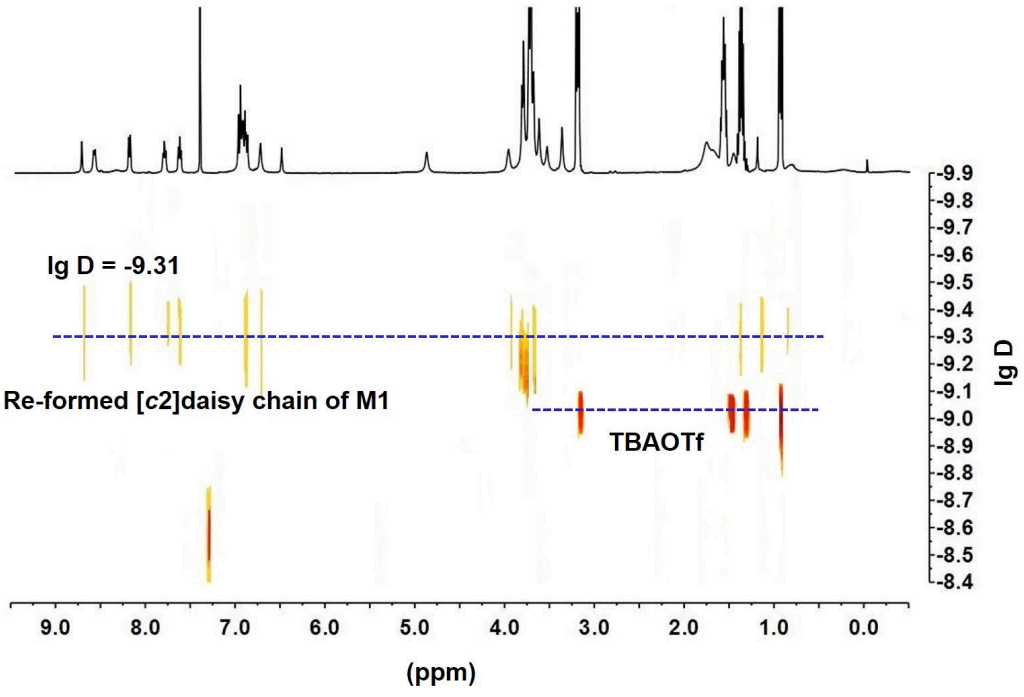

Figure S27. The diffusion coefficient (lg D) (600 MHz, $CDCl_3$, 298K) spectrum of **M1** (2 mM), TBACl (4 mM) and AgOTf (8.0 equiv.).

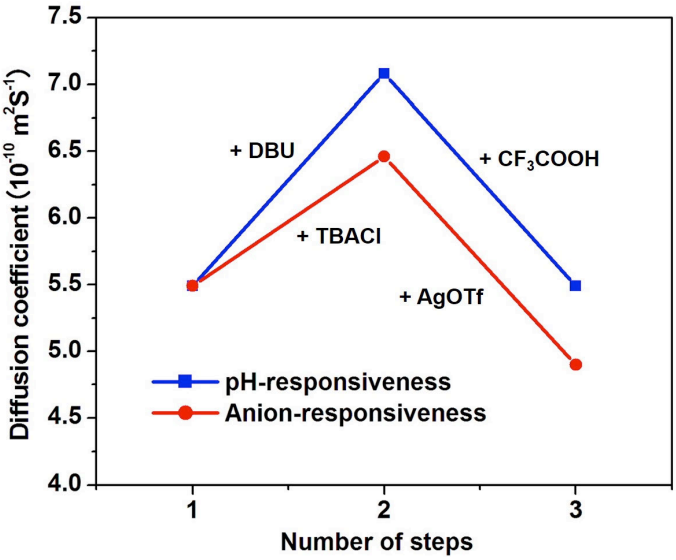

Figure S28. Diffusion coefficient of the solution of **M1** (2 mM, in $CDCl_3$, 298 K) upon the stepwise addition of DBU (2 mM) and CF_3COOH (10 mM) or TBACl (4 mM) and AgOTf (8.0 equiv.).

11. Synthesis of the ditopic pillar[5]arene derivatives

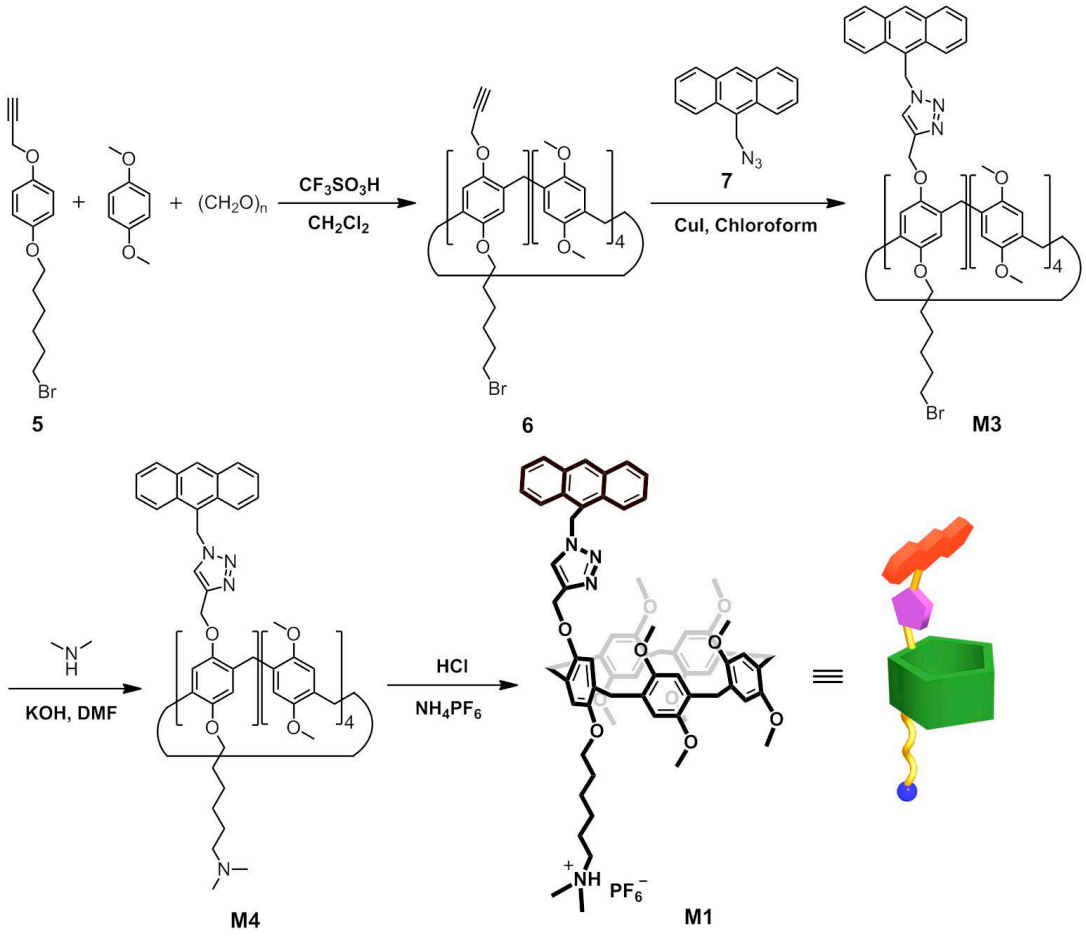

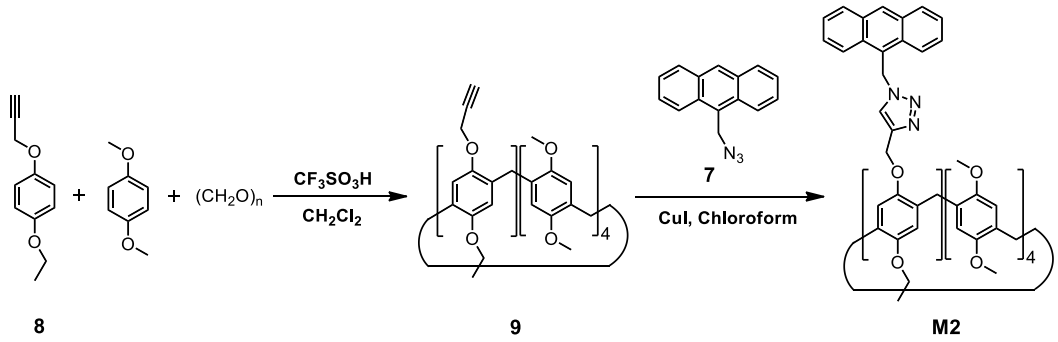

Scheme S1. Synthetic routes to pillarene derivatives

Compounds 5 and **8** were prepared according to the previous literature.[S8]

Synthesis of compound **6**.

Paraformaldehyde (1.62 g, 54 mmol) was added to a solution of 1-((6-bromohexyl)oxy)-4-(prop-2-yn-1yloxy)benzene **5** (1.87 g, 6 mmol) and 1,4-dimethoxybenzene (4.14 g, 30 mmol) in dichloromethane (120 mL). Then, TfOH (0.33 mL, 5 mol%) was added to the solution and the mixture was stirred at room temperature (approximately 25 °C) for 24h. The mixture was poured into aqueous NH_4Cl solution (120 mL), the organic layer was collected and aqueous layer was extracted with CH_2Cl_2 three times. The combined organic layers were dried over anhydrous Na_2SO_4, filtered, and then the solvent was removed by rotary evaporation. The crude product was purified by flash column chromatography with an appropriate eluting solvent (petroleum ether/ethyl acetate 30:1) to get the desired product **6** as a white solid (0.83 g, 15%). ^{1}H NMR (300 MHz, $CDCl_3$, 298 K) δ = 6.93−6.76 (m, 10H), 4.61 (s, 2H), 3.79−3.65 (m, 34H), 2.31 (s, 1H), 1.41 (s, 4H), 1.26 (s, 2H), 0.84 (s, 2H), 0.34 (s, 2H). ^{13}C NMR (125 MHz, $CDCl_3$, 298 K) δ (ppm): 151.0, 150.8, 150.7, 150.3, 150.2, 150.1, 148.7, 128.1, 128.0, 127.8, 113.9, 113.3, 113.0, 79.4, 74.6, 56.1, 55.7, 55.4, 55.3, 55.2, 29.6, 29.0, 27.7, 24.0, 22.6, 14.1. MS (MALDI–TOF) calcd for $C_{52}H_{59}O_{10}Br$, *m/z* = 924.6629, found *m/z* = 924.6645 $[M]^+$, 947.6567 $[M+Na]^+$, 963.6547 $[M+K]^+$.

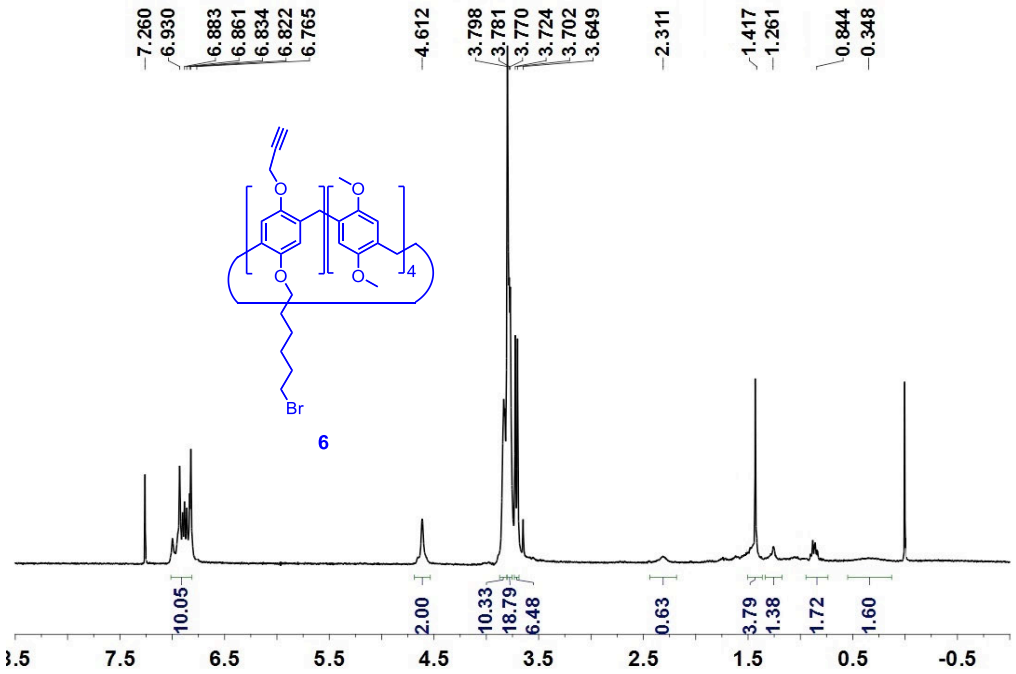

Figure S29. ^{1}H NMR spectrum ($CDCl_3$, 298 K, 300 MHz) of **6.**

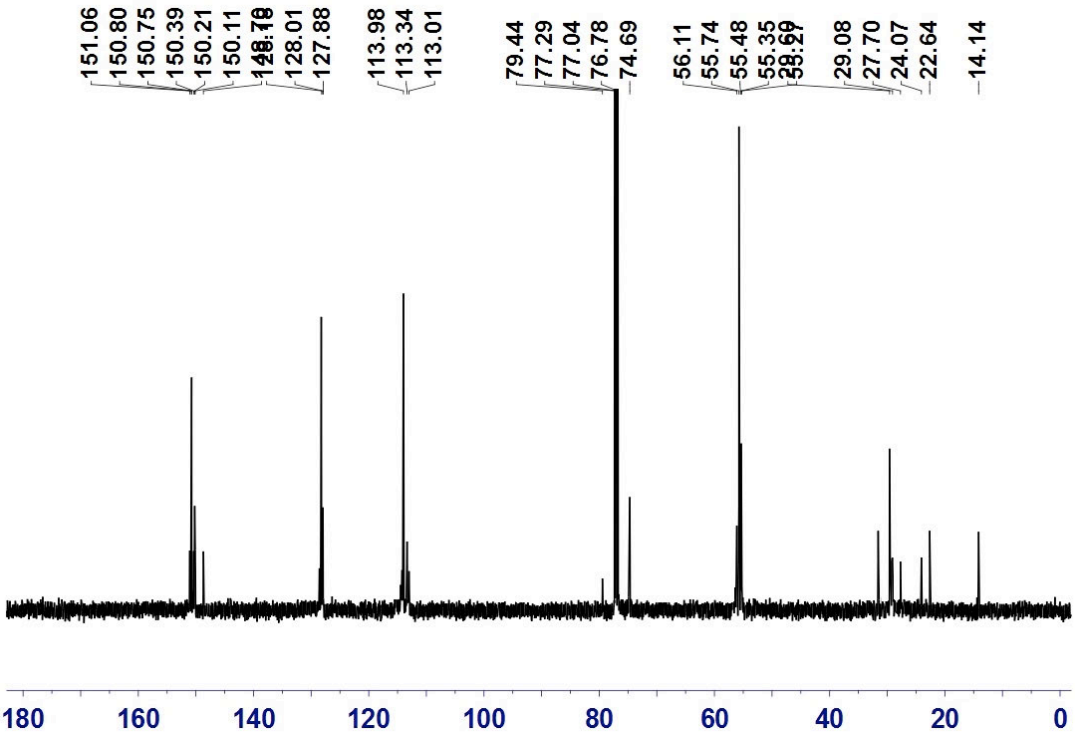

Figure S30. ^{13}C NMR spectrum ($CDCl_3$, 298 K, 125 MHz) of **6**.

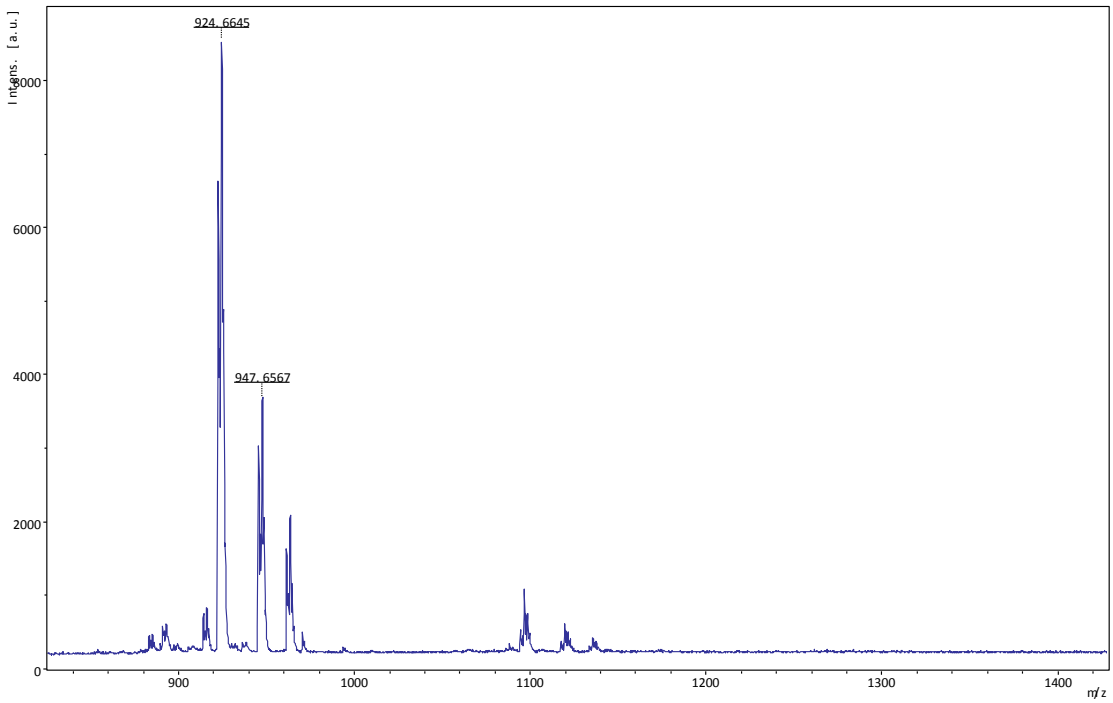

Figure S31. MS (MALDI-TOF) of **6**.

Synthesis of compound **M3**.

To a stirred mixture of **6** (0.74 g, 0.8 mmol), **7** (0.22 g, 0.96 mmol) and CuI (16 mg, 0.08 mmol) in $CHCl_3$ (25 mL) was added 2,6-lutidine (94 μL, 0.8 mmol) at room temperature. After stirring for 18 h at room temperature, the reaction mixture was diluted with CH_2Cl_2 (25 mL) and then with aqueous NH_4Cl solution (50 mL). The mixture was stirred for an additional 15 minutes and two layers were separated. The aqueous layer was extracted with CH_2Cl_2 (20 mL × 3) and the combined organic layers were dried over anhydrous Na_2SO_4, concentrated *in vacuo*. The crude residue was purified by flash column chromatography (Petroleum ether/Ethyl acetate, 2:1) to give the desired product **M3** as a yellow solid (0.78 g, 85%). ^{1}H NMR (500 MHz, $CDCl_3$, 298 K) δ (ppm): 8.60 (s, 1H), 8.37 (d, J = 7 Hz, 2H), 8.37 (d, J = 7 Hz, 2H), 8.10 (d, J = 7 Hz, 2H), 7.60-7.54 (m, 4H), 7.33 (s, 1H), 6.99-6.59 (m, 12H), 4.98 (s, 2H), 3.74-3.62 (m, 32 H), 3.23 (s, 2H), 1.63 (s, 2H), 1.34-1.26 (m, 8H), 1.17-1.07 (m, 2H) . ^{13}C NMR (125 MHz, $CDCl_3$, 298 K) δ (ppm): 151.0, 150.7, 150.3, 150.1, 150.0, 149.9, 149.1, 145.2, 141.6, 131.4, 127.7, 125.4, 121.9, 114.0, 113.2, 113.0, 65.5, 62.5, 53.0, 46.5, 29.5, 29.1, 28.9, 22.6, 14.1. MS (MALDI–TOF) calcd for $C_{67}H_{70}O_{10}N_3Br$, m/z = 1157.0109, found m/z = 1156.9011 $[M]^+$, 1179.9459 $[M+Na]^+$, 1196.0583 $[M+K]^+$.

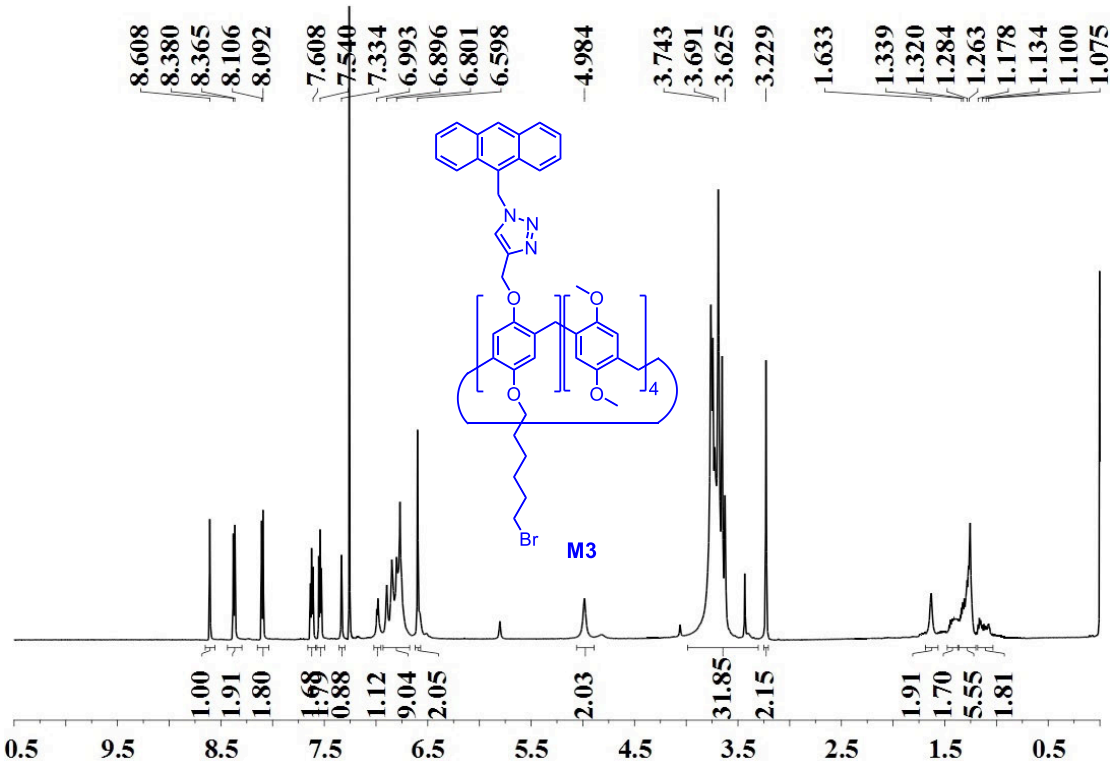

Figure S32. ^{1}H NMR spectrum ($CDCl_3$, 298 K, 500 MHz) of **M3.**

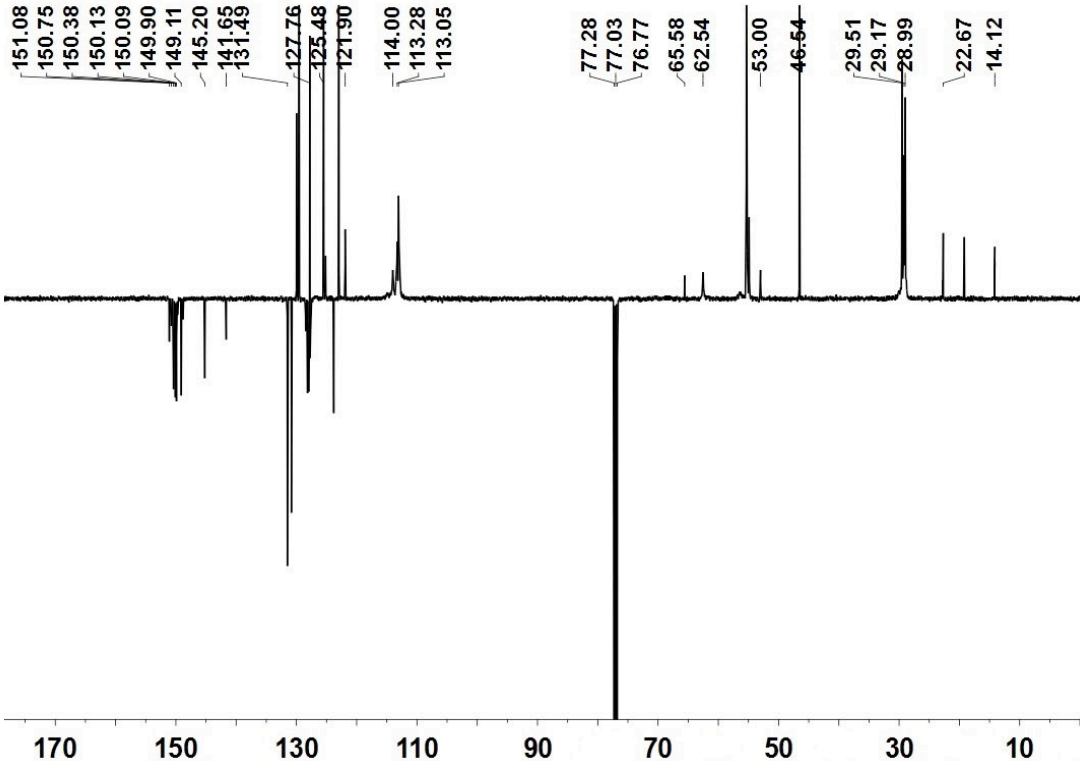

Figure S33. ^{13}C NMR spectrum ($CDCl_3$, 298 K, 125 MHz) of **M3.**

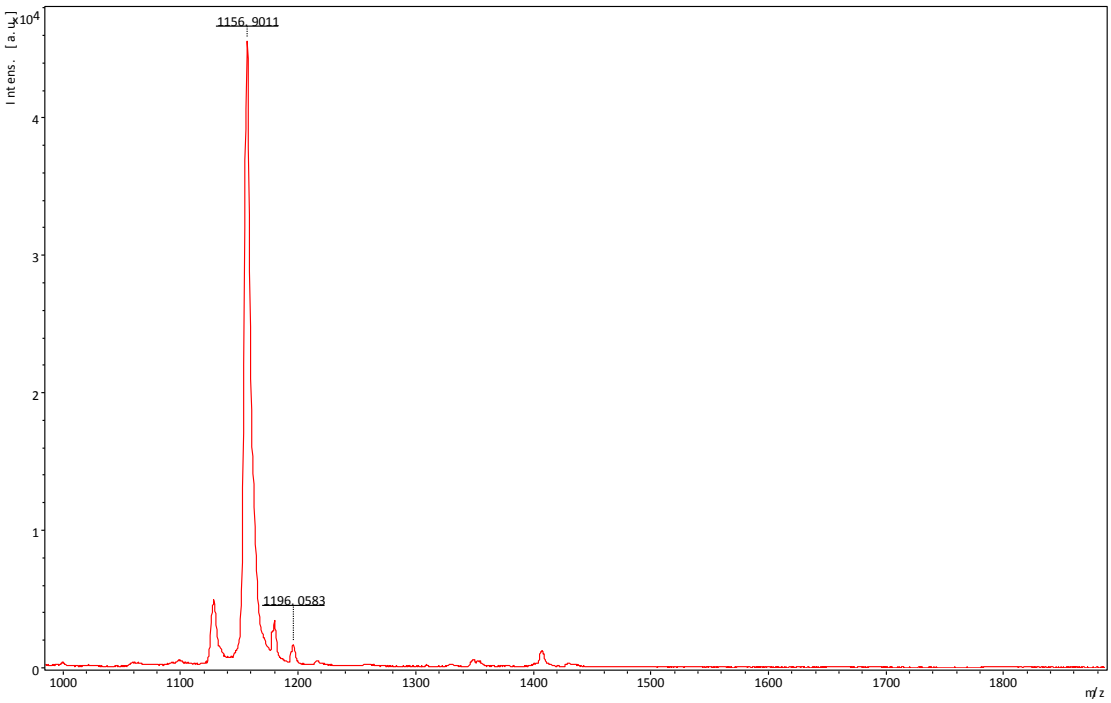

Figure S34. MS (MALDI-TOF) of **M3**.

Synthesis of compound **M4**.

N,N-dimethylamine (1.2 mmol) and potassium hydroxide (0.067 g, 1.2 mmol) were added to a solution of compound **M3** (0.69 g, 0.6 mmol) in DMF (10 mL). Then, the reaction mixture was stirred at 50 °C for 4h, cooled to room temperature and added to CH_2Cl_2 (30 mL). The solution was washed with H_2O three times. The organic layer was removed under vacuum and purified by column chromatography (DCM / EtOAc, 20:1) to afford compound **M4** as a yellowish solid (0.43 g, 64%). ^{1}H NMR (500 MHz, $CDCl_3$, 298 K) δ (ppm): 8.58 (s, 1H), 8.35 (d, J = 7 Hz, 2H), 8.07 (s, 2H), 7.60-7.54 (m, 4H), 7.30 (s, 1H), 6.74-6.67 (m, 12H), 4.83 (s, 2H), 3.78-3.53 (m, 34H) 3.17 (s, 3H), 2.26-2.24 (m, 2H), 2.22 (s, 6H), 1.76 (s, 2H), 1.54-1.37 (m, 6H). ^{13}C NMR (125 MHz, $CDCl_3$, 298 K) δ (ppm): 150.6, 149.3, 131.4, 128.1, 127.7, 122.9, 115.7, 114.7, 114.0, 113.9, 113.8(8), 113.8(0), 68.3, 55.7, 55.3, 46.5, 45.5, 29.7, 29.4, 27.7, 26.3, 11.4. MS (MALDI-TOF) calcd for $C_{69}H_{76}O_{10}N_4$, *m/z* = 1120.6570, found *m/z* = 1120.6553 $[M]^+$.

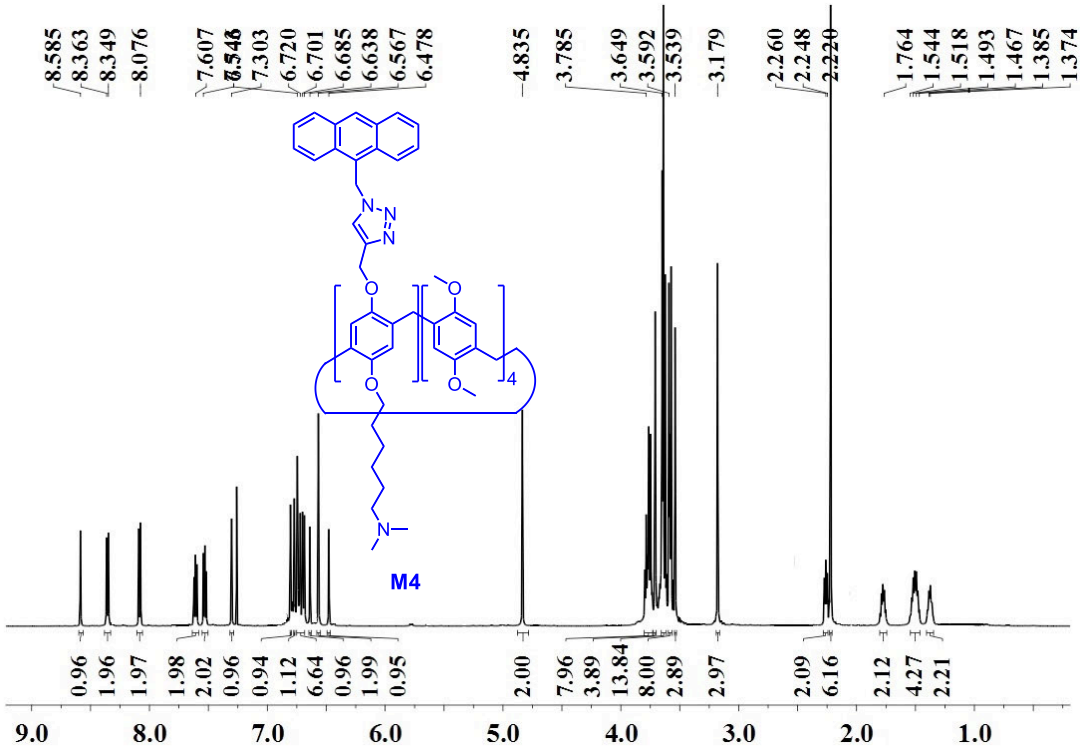

Figure S35. ^{1}H NMR spectrum ($CDCl_3$, 298 K, 500 MHz) of **M4.**

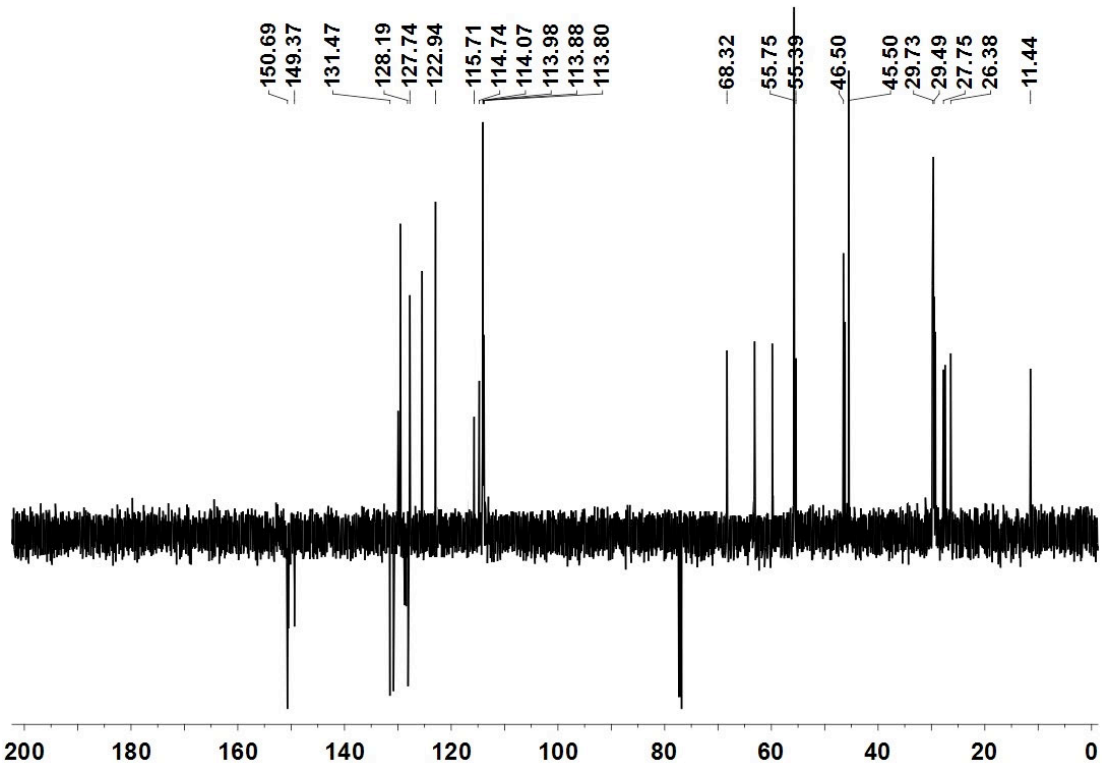

Figure S36. ^{13}C NMR spectrum ($CDCl_3$, 298 K, 125 MHz) of **M4.**

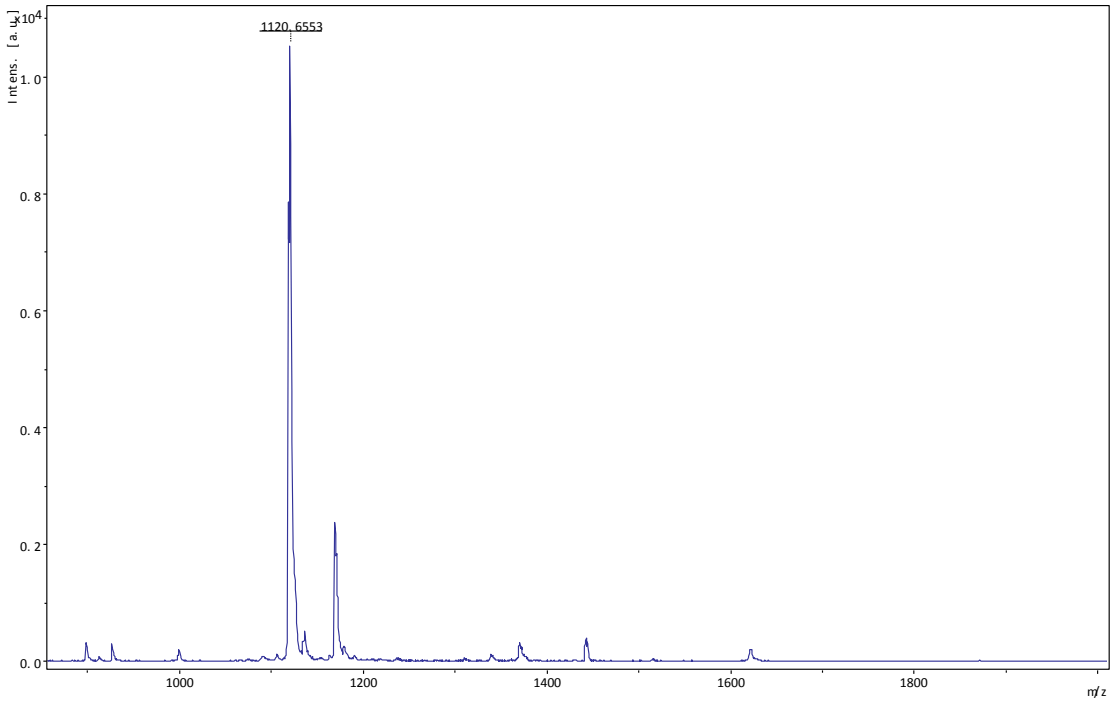

Figure S37. MS (MALDI-TOF) of **M4**.

Synthesis of compound **M1**.

To the solution of **M2** (0.336 g, 0.3 mmol) in DCM / MeOH (5 mL) was added HCl aqueous to adjust pH < 2, then a saturated aqueous solution of NH_4PF_6 (5 equiv.) was added to the mixture. The resulting solution was stirred at room temperature for 2 hours. The solvent was removed in *vacuo*, the residue was suspended in water (10 mL). The precipitate was filtered off and washed with deionized water to afford compound **M1** as a yellow solid (0.266 g, 75 %). ^{1}H NMR (500 MHz, $CDCl_3$, 298 K) δ (ppm): 8.58 (d, *J* = 9 Hz, 2H), 8.56 (s, 1H), 8.07 (d, *J* = 9 Hz, 2H), 7.87 (s, 1H), 7.69-7.67 (m, 2H), 7.55-7.52 (m, 2H), 7.09 (s, 1H), 6.91-6.78 (m, 8H), 6.62 (s, 3H), 4.95 (s, 2H), 3.88-3.70 (m, 34H), 3.16 (s, 3H), 1.79 (s, 5H), 1.62 (s, 3H), 1.42-1.38 (m, 2H), 0.07 (s, 3H), -0.77 (s, 1H), -1.16 (s, 1H). ^{13}C NMR (125 MHz, $CDCl_3$, 298 K) δ (ppm): 151.1, 150.8, 150.7, 150.6, 150.3, 150.2, 129.2, 127.6, 124.6, 123.4, 114.8, 113.8, 113.5, 56.1, 55.6, 55.3, 46.4, 46.1, 42.8, 29.1, 21.9. MS (MALDI-TOF) calcd for $C_{69}H_{77}O_{10}N_4$, *m/z* = 1122.2298 $[M\text{-}PF_6]^+$, found *m/z* = 1123.2186 $[M\text{-}PF_6\text{+}H]^+$, 2246.8156 (dimer of M1).

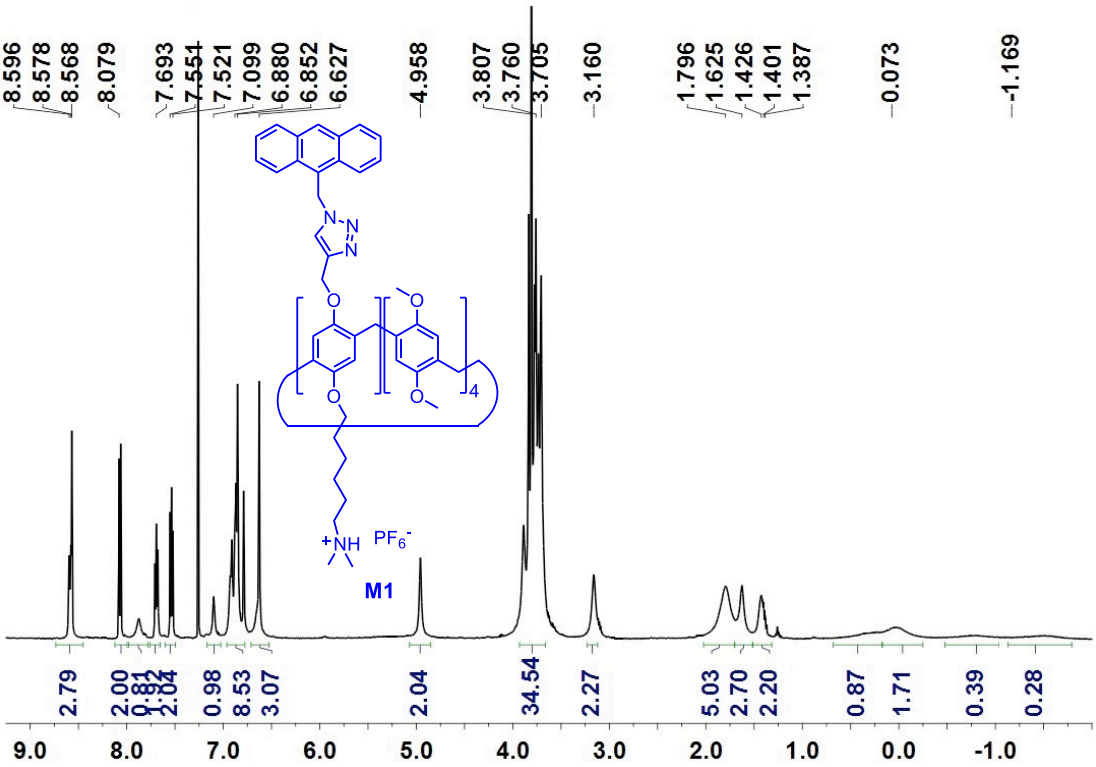

Figure S38. ^{1}H NMR spectrum (500 MHz, $CDCl_3$, 298 K) of **M1.**

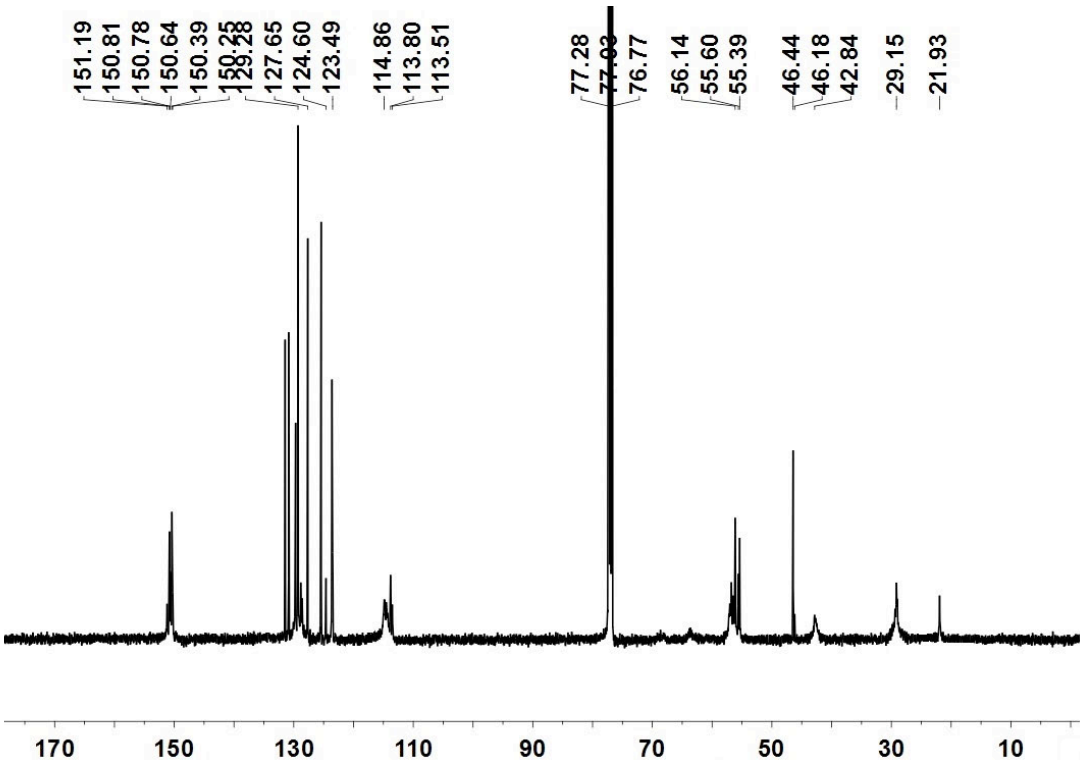

Figure S39. ^{13}C NMR spectrum ($CDCl_3$, 298 K, 125 MHz) of **M1.**

[M1-PF_6+H]

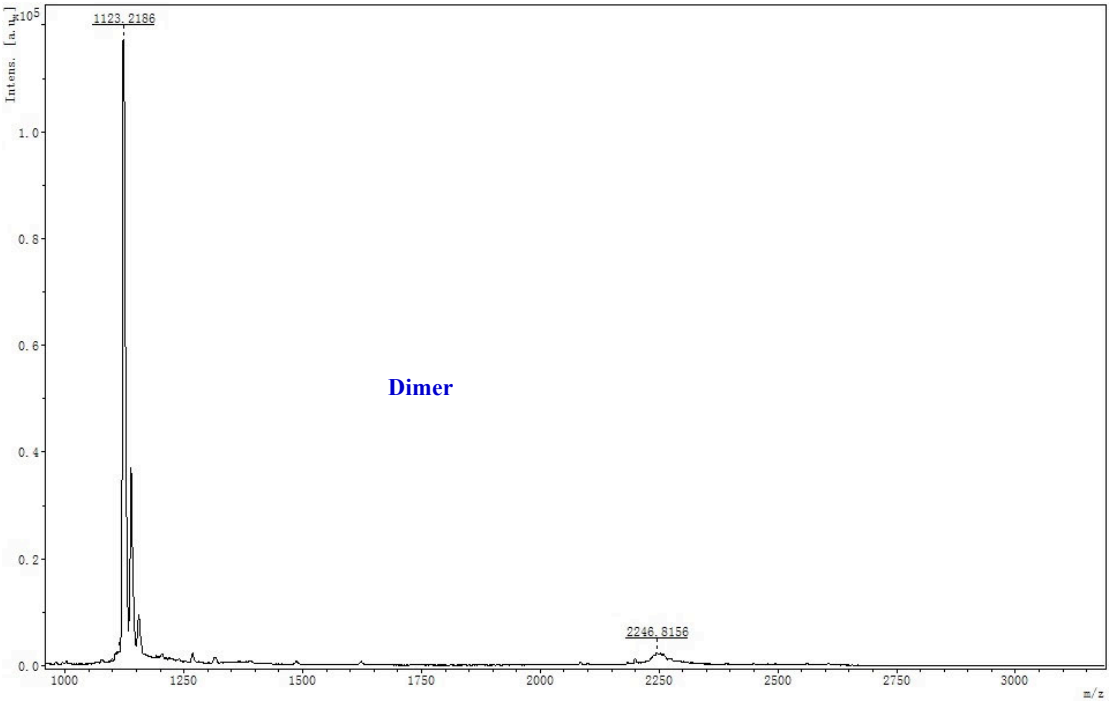

Figure S40. MS (MALDI-TOF) of **M1**.

Synthesis of compound **9**.

Paraformaldehyde (1.08 g, 36 mmol) was added to a solution of 1-ethoxy-4-(prop-2-yn-1yloxy)benzene **8** (0.70 g, 4 mmol) and 1,4-dimethoxybenzene (2.76 g, 20 mmol) in dichloromethane (100 mL). Then, TfOH (0.22 mL, 5 mol%) was added to the solution and the mixture was stirred at room temperature (approximately 25 °C) for 24h. The mixture was poured into aqueous NH_4Cl solution (100 mL), the organic layer was collected and aqueous layer was extracted with CH_2Cl_2 three times. The combined organic layers were dried over anhydrous Na_2SO_4, filtered, and then the solvent was removed by rotary evaporation. The crude product was purified by flash column chromatography with an appropriate eluting solvent (petroleum ether/ethyl acetate 40:1) to get the desired product **9** as a white solid (0.378 g, 12%). ^{1}H NMR (500 MHz, $CDCl_3$, 298 K) δ (ppm): 6.80-6.73 (m, 10H), 4.44 (d, J = 4 Hz, 2H), 3.79-3.64 (m, 36H), 1.95 (d, J = 4 Hz, 1H), 1.29 (t, J = 11 Hz, 3H). ^{13}C NMR (125 MHz, $CDCl_3$, 298 K) δ (ppm): 150.7(8), 150.7(7), 150.7(4), 150.7(2), 150.6, 150.4, 148.7, 128.4, 128.2, 128.1, 114.2, 114.0, 113.9(2), 113.9(0), 113.8, 79.0, 74.6, 63.8, 55.7(8), 55.7(3), 52.8, 30.1, 29.6(7), 29.6(2), 29.5, 29.2, 15.0.

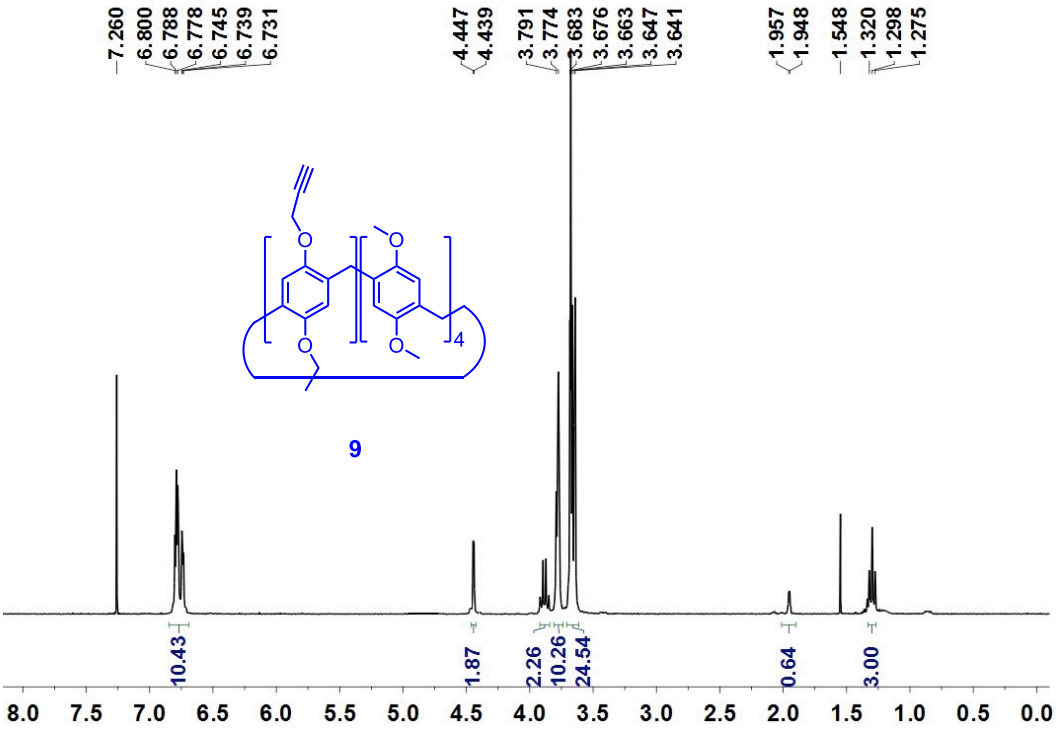

Figure S41. ^{1}H NMR spectrum (500 MHz, $CDCl_3$, 298 K) of **9.**

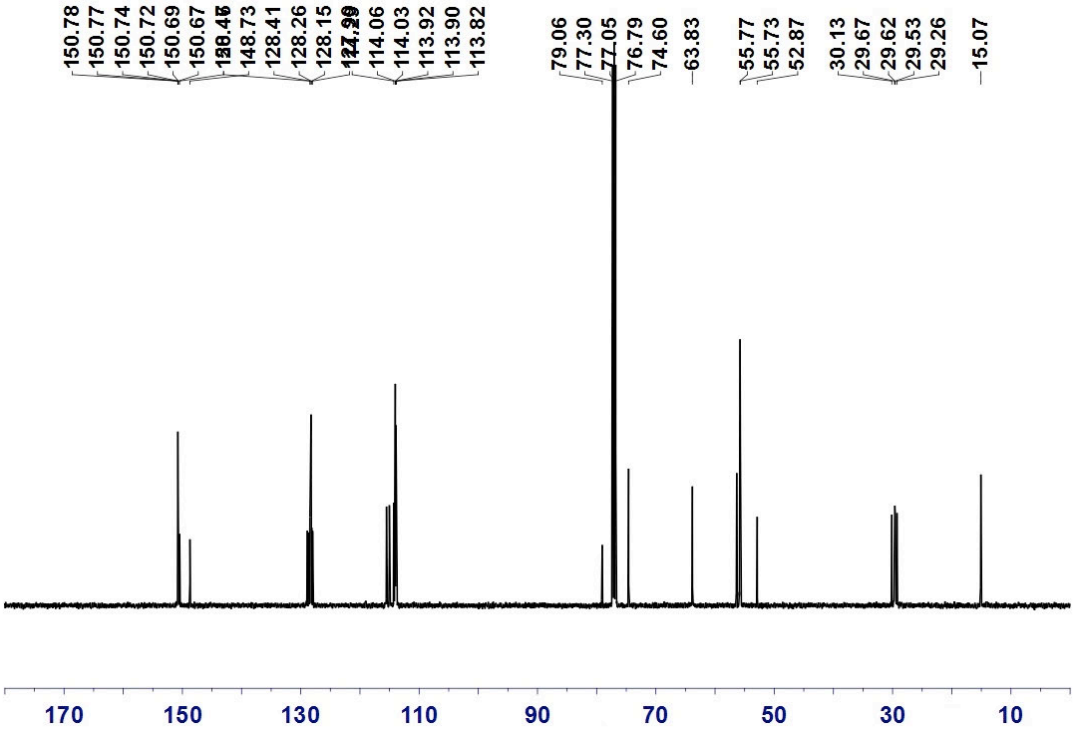

Figure S42. ^{13}C NMR spectrum ($CDCl_3$, 298 K, 125 MHz) of **9.**

Synthesis of compound **M2**.

To a stirred mixture of **9** (0.236 g, 0.3 mmol), **7** (84 mg, 0.36 mmol) and CuI (6 mg, 0.03 mmol) in $CHCl_3$ (5 mL) was added 2,6-lutidine (35 μL, 0.3 mmol) at room temperature. After stirring for 18 h at room temperature, the reaction mixture was diluted with CH_2Cl_2 (15 mL) and then with aqueous NH_4Cl solution (20 mL). The mixture was stirred for an additional 15 minutes and two layers were separated. The aqueous layer was extracted with CH_2Cl_2 (10 mL × 3) and the combined organic layers were dried over anhydrous Na_2SO_4, concentrated *in vacuo*. The crude residue was purified by flash column chromatography (Petroleum ether/Ethyl acetate, 5:1) to give the desired compound **M2** as a light-yellow solid (245 mg, 80%). ^{1}H NMR (500 MHz, $CDCl_3$, 298 K) δ (ppm): 8.59 (s, 1H), 8.35 (d, J = 7 Hz, 2H), 8.08 (d, J = 7 Hz, 2H), 7.60 (t, J = 6.5 Hz, 2H), 7.52 (t, J = 6.5 Hz, 2H), 7.28 (s, 1H), 6.74-6.57 (m, 9H), 6.45 (s, 1H), 4.86 (s, 2H), 3.77-3.50 (m, 34H), 3.22 (s, 3H), 1.16 (t, J = 6.0 Hz, 3H). ^{13}C NMR (125 MHz, $CDCl_3$, 298 K) δ (ppm): 150.8(7), 150.8(2), 150.7, 150.6, 150.5, 149.2, 145.1, 129.5, 128.1, 127.7, 122.9, 114.1, 114.0, 113.9(9), 113.9(1), 63.4, 63.3, 55.5, 46.5, 29.7, 29.6, 29.5, 29.3, 14.8. MS (MALDI-TOF) calcd for $C_{63}H_{63}O_{10}N_3$, m/z = 1022.1855, found m/z = 1022.1849 [M], 1145.1859 $[M+Na]^+$.

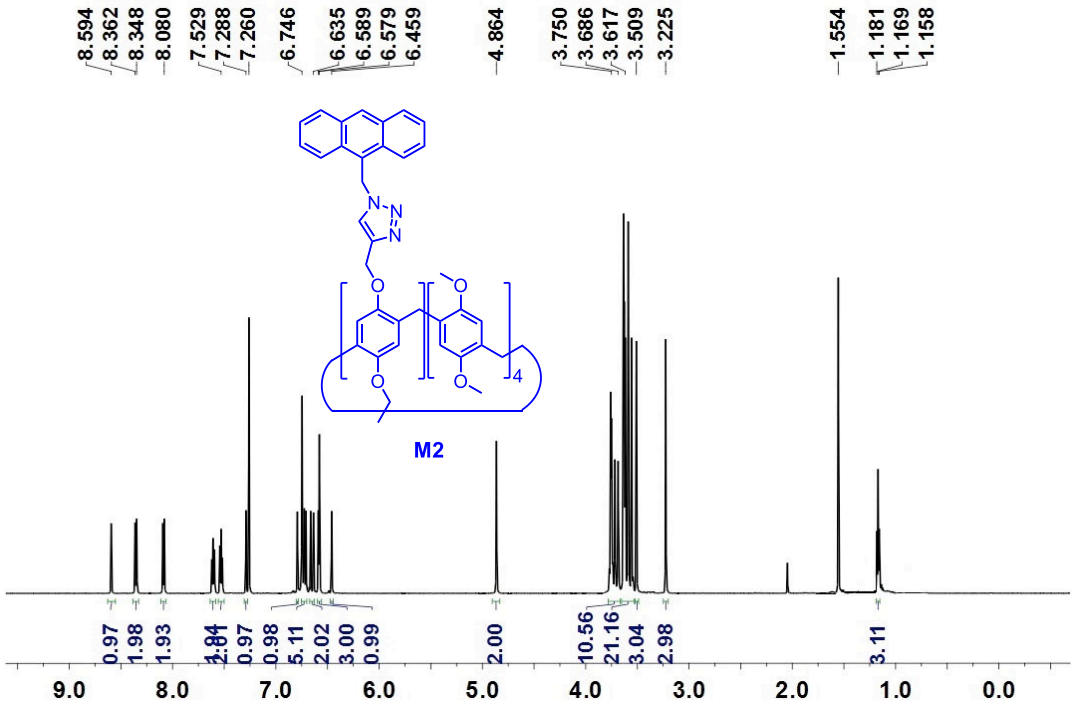

Figure S43. ^{1}H NMR spectrum (500 MHz, $CDCl_3$, 298 K) of **M2.**

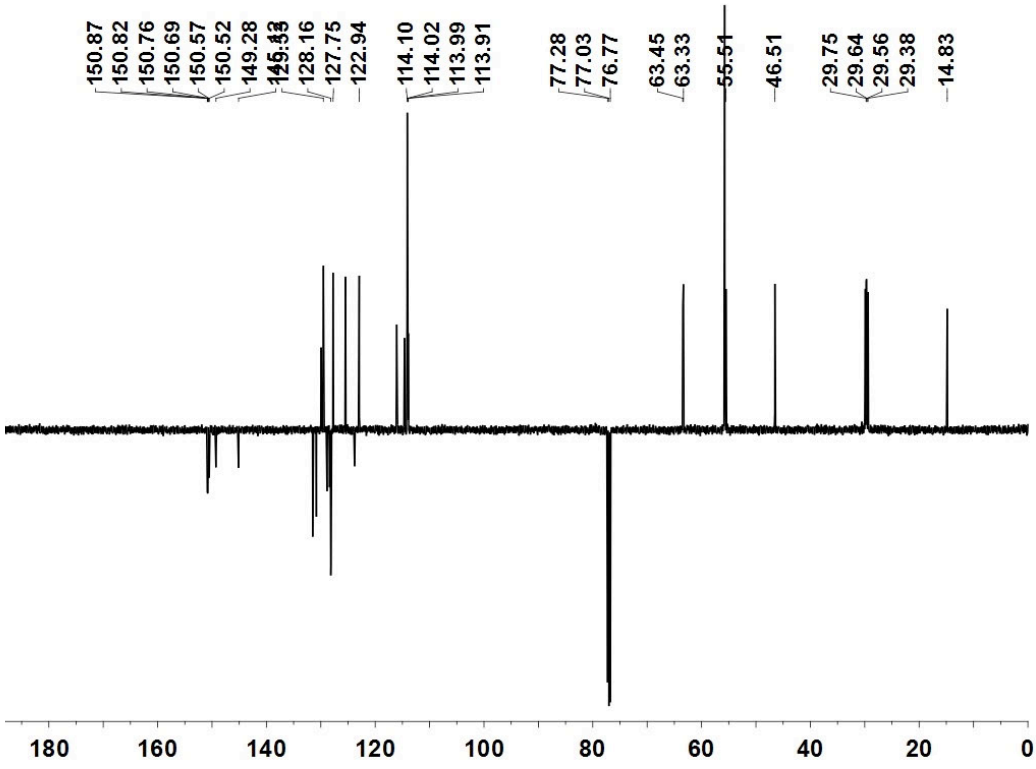

Figure S44. ^{13}C NMR spectrum ($CDCl_3$, 298 K, 125 MHz) of **M2.**

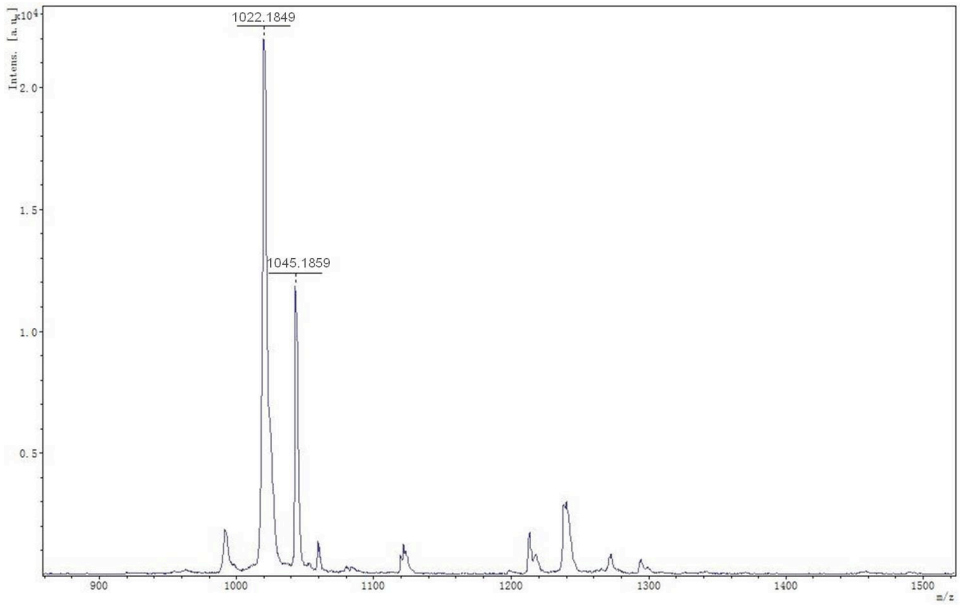

Figure S45. MS (MALDI-TOF) of **M2**.

12. References

S1. C. Li, K. Han, J. Li, Y. Zhang, W. Chen, Y. Yu and X. Jia, *Chem. Eur. J.*, 2013, **19**, 11892-11897.

S2. K. Wang, C.-Y. Wang, Y. Wang, H. Li, C.-Y. Bao, J.-Y. Liu, S. X.-A. Zhang and Y.-W. Yang, *Chem. Commun.*, 2013, **49**, 10528-10530.

S3. (a) Y. Liu, Z. Fan, H.-Y. Zhang and C.-H. Diao, *Org. Lett.*, 2003, **5**, 251-254; (b) Y. Liu, Z. Fan, H.-Y. Zhang, Y.-W. Yang, F. Ding, S.-X. Liu, X. Wu, T. Wada and Y. Inoue, *J. Org. Chem.*, 2003, **68**, 8345-8352.

S4. N. L. Strutt, H. Zhang, M. A. Giesener, J. Lei and J. F. Stoddart, *Chem. Commun.*, 2012, **48**, 1647-1649.

S5. T. Ogoshi, S. Kanai, S. Fujinami, T.-a. Yamagishi and Y. Nakamoto, *J. Am. Chem. Soc.*, 2008, **130**, 5022-5023.

S6. K. Suzuki, A. Kobayashi, S. Kaneko, K. Takehira, T. Yoshihara, H. Ishida, Y. Shiina, S. Oishi and S. Tobita, *Phys. Chem. Chem. Phy.*, 2009, **11**, 9850-9860.

S7. H. Zheng, Q. Wang, Y. Long, H. Zhang, X. Huang and R. Zhu, *Chem. Commun.*, 2011, **47**, 10650-10652.

S8. M. Srinivasan, S. Sankararaman, H. Hopf, I. Dix and P. G. Jones, *J. Org. Chem.*, 2001, **66**, 4299-4303.